Supporting Information

-

A ^{15}N-NMR based approach for amino acids based ^{13}C-metabolic flux analysis of metabolism

Pierre Millard, Edern Cahoreau, Maud Heuillet, Jean-Charles Portais, and Guy Lippens*

LISBP, Université de Toulouse, CNRS, INRA, INSA, Toulouse, France

*glippens@insa-toulouse.fr

Table of contents

1) Sample preparation

Starting from 25mg ^{15}N,^{13}C labeled algal extract (Cambridge Isotope Laboratories, Tewksbury, USA), we fully hydrolysed it by overnight incubation in 6N HCl at 100°C. The resulting sample was dried by evaporation, and resuspended in water with 0.1% HCl.

As for the bacterial samples, *E. coli* K12 bacteria were grown on a minimal medium containing 1g/l $^{15}NH_4Cl$ (Cambridge Isotope Laboratories, Tewksbury, USA) as sole nitrogen source, and 3g/l U-^{13}C glucose as sole carbon source for the uniformly labelled sample. Labeling with an equiprobable^{13}C-enrichment at every position (the "Pascal triangle" (PT) sample was obtained by growing cells on acetate (3g/l) as sole carbon source, using the 4 isotopomers of acetate in exactly the same ratio as verified by NMR spectroscopy. The resulting sample, which contains all the isotopomers of each metabolite in equal proportions, was previously developed as a standard for mass spectrometry [1]. The proportions of each acetate isotopomer in the label input were measured by 1D ^1H NMR, using a zgpr30 sequence with a relaxation delay of 10 seconds. The experimental isotopomer distribution (^{12}C-acetate : 25.0±0.5%, 1-^{13}C-acetate : 25.0±0.5%, 2-^{13}C-acetate : 25.2±0.5%, U-^{13}C-acetate : 24.8±0.5%) corresponds to a molecular ^{13}C-enrichment of 49.9±0.7%.

2) Mass spectrometry

Labeling of the PT sample was verified in an independent manner by liquid chromatography (Ultimate 3000 HPLC system, Dionex, CA, USA) coupled to a high resolution mass spectrometer (LTQ-Orbitrap Velos, Thermo Fisher Scientific, Waltham, MA, USA) as described in Millard et al, 2014. Because this PT sample was fully labeled with ^{15}N, the exact mass of the ^{13}C-isotopologues has to take into account the ^{15}N labeling next to the number of incorporated ^{13}C nuclei. A mass spectrometer resolution of 60 000 was used, which allows to

differentiate the ^{13}C incorporation from ^{15}N incorporation for this range of masses. The resulting percentages of ^{13}C incorporation for the different amino acids according to this mass spectrometry assay confirmed that the sample obeyed the Pascal triangle distribution.

3) NMR spectroscopy

Samples contain typically the hydrolysate of 15mg of bacterial slurry after complete hydrolysis. They were resuspended in 200µl of H_2O with 0.1% HCl, and introduced in a 3mm tube. This tube was inserted in a 5mm regular NMR tube filled with D_2O for locking purpose, and 10mM TMSP for proton referencing.

NMR experiments were performed on a Bruker Avance III spectrometer operating at 800MHz proton frequency and equipped with a TCI cryogenic probe head. Temperature of the samples was 273.2K.

HISQC – The HISQC sequence (Figure S1) is the same as the one developed for the observation of the Lysine side chains (ref. 16). The nitrogen carrier is put at 34ppm, with a spectral window of 20ppm. Delays Δ and Δ' in the refocused HSQC sequence correspond to 2.7ms and 1.3ms, respectively, and take into account the coupling of the protons to one single nitrogen, whereas the nitrogen is coupled to three protons. During the nitrogen evolution, one avoids the evolution of $H_zN_{x,y}$ terms by continuous decoupling of the protons by a Waltz16 train. Nitrogen decoupling during the acquisition is obtained by a garp decoupling sequence.

HNCACB - The HNCACB experiment (Figure S2-1) is based on the pulse sequence originally designed for the assignment of $^{15}N/^{13}C$ labelled proteins.[2,3] Modifications concern the d21 delay wherein the antiphase H_zN_x term refocuses to a pure nitrogen term. To account for the presence of three protons rather than one on the ^{15}N nitrogen of free amino acids, this refocusing delay d21 is set to 2.4ms. The delay d23 to generate antiphase N_xCO_z magnetization is set to 36ms. Other delays are Δ=2.3ms, d28=3.6ms, 2*d30 = d23. Carbon chemical shift encoding is done by incrementing the t_1 delay, whereas ^{15}N encoding is done in a constant time manner by incrementing d10 and d29 while simultaneously decrementing d30. Phase selection in the indirect carbon dimension follows the States-TPPI scheme, implemented by incrementing the phases of the 90° carbon pulses following the carbon evolution (Φ_9 & Φ_{10}). Selection of the x or y component of the nitrogen term follows the same States-TPPI scheme, and is obtained by incrementing Φ_5 by 90°.

Proton hard pulses are delivered with 18W power, leading to a 9.5µs 90° hard pulse (open rectangles) or 19µs 180° pulse (filled rectangles). The water flip-back pulse (shaded rectangle) was implemented as a square 1ms pulse with 1.6mW power level. Proton decoupling was performed with a DIPSI2 pulse train with a 60µs 90°pulse. The decoupling sequence is preceded and followed by a 90° pulse at the same power level to align the water along the DIPSI2 axis.

Nitrogen hard pulses are delivered with 160W, leading to a 34µs 90° hard pulse (open rectangles) or 68µs 180° pulse (filled rectangles). Nitrogen decoupling during the acquisition was performed with a garp4 pulse train with a 340µs 90°pulse.

Carbon pulses are delivered as shaped pulses. The 90° pulses (open shapes) are implemented as Gaussian cascade Q3 pulses of 170µs delivered with 151.4W. Parameters for the 180° pulses (filled shapes) are Gaussian cascade Q5 pulses of 213µs with 154.9W. The carbon transmitter is centered at 41ppm, and pulses on the carbonyl carbons are implemented as off-resonance pulses centered at 176ppm.

Gradient pulses were implemented as 1ms smoothed square pulses. Gradient strengths are 50% (G_1), 40% (G_2), 60% (G_3) and 30% (G_4) of the maximal gradient strength. All gradients are followed by a 200µs recovery delay.

Phases of the pulses are x when nothing is indicated. For the other phases, we have Φ_2 = x, Φ_3 = 8*x, 8*-x, Φ_5 = x x –x –x, Φ_6 = -x, Φ_7 = -y, Φ_8 = x x –x –x, Φ_9 = -y y, Φ_{10} = x –x x –x –x x –x x, acquisition phase = x –x –x x –xx x –x –x x x –xx –x-xx.

The experiment was acquired as a complex matrix of 4k x 96 x 320 points for a spectral width of 13.95 x 26 x 70ppm in the ^{1}H, ^{15}N, ^{13}C dimensions respectively. With 4 scans per increment and a relaxation delay of 1s, the total time was 1day 23 hours and 43minutes. After zero filling and apodization with a squared sine bell in the three dimensions, it was transformed as a matrix of 4k x 1k x 1k points. Processing was done with the Bruker Topspin software.

HNCA - The HNCA experiment to measure the conditional ^{13}CO incorporation (Figure 3) was a modification of the classical HNCA experiment, with exactly the same modifications as for the HNCACB experiment. The experiment as performed in its 3D version as a matrix of 4k x 32 x 1024 points, for a spectral width of 13.95 x 8.7 x 11ppm in the ^{1}H, ^{15}N, ^{13}C dimensions respectively. The carbon carrier was set to 53.3ppm. With 2 scans per increment and a relaxation delay of 1s, the total time was 1day 3 hours and 10minutes. After zero filling and apodization with a squared sine bell in the three dimensions, it was transformed as a matrix of 4k x 256 x 4k points. Processing was done with the Bruker Topspin software. The same

experiment was repeated as a 2D ^{1}HN, ^{13}Ca plane with the same spectral parameters but without ^{15}N evolution. Varying the d1 delay from 1s, 2s, 4s to 6s led to acquisition times of 1h42m, 2h50m, 5h7m and 3h43m, whereby all experiments were done with 4scans/increment except for the last one (d1=6s) with 2scans/increment.

HA-CO - The Hα-^{13}CO experiment (Figure S6-4) is based on the original ^{1}H, ^{13}C HSQC pulse sequence with sensitivity enhancement[4]. Modifications are the Δ delay of 34ms, to allow evolution of the Hα term into a $H\alpha_y CO_z$ antiphase term under the 7.3Hz Hα-^{13}CO coupling constant. The delay Δ3 is set to 1/8J(^{1}Hα-^{13}CO) or 17ms. A correction factor has to take into account the additional differential relaxation of the ^{12}C/^{13}C linked Hα protons during the delay of 4*Δ + 2xΔ3 (see Data analysis). The 180° proton pulse during this INEPT block is implemented as a 2ms Gaussian cascade Q3 shaped pulse with maximal B_1 field of 330Hz, covering 0.5ppm at 800MHz. This pulse is selective such as not to excite the Hβ terms, thereby effectively refocusing the Hα-Hβ coupling constant. The carbonyl 180° pulse during the INEPT block is equally implemented as a shaped Gaussian cascade Q3 pulses of 170µs delivered with 151.4W and centered at171ppm. Other delays are Δ1 = 1.22ms. During the carbon evolution, ^{13}Cα and ^{15}N coupling constants to the ^{13}CO are decoupled by insertion of the corresponding 180° pulses. Phase selection in the indirect dimension is done by the echo/anti-echo method, by inverting the gradient G_1 and incrementing the phase Φ_5 by 180°.

Gradient pulses were implemented as 1ms smoothed square pulses unless G_2 which had a duration of 600µs. Gradient strengths are 80% (G_1), 11% (G_2), -5% (G_3) and 20.1% (G_4) of the maximal gradient strength. All gradients are followed by a 200µs recovery delay.

Phase of the pulses is x when nothing is indicated. For the other phases, we have Φ_2 = y, Φ_3 = x -x, Φ_4 = x x –x –x, Φ_5 = y y –y -y, acquisition phase = x –x –x x.

The experiment was acquired as a complex matrix of 8k x 256 points for a spectral width of 12.02 x 5ppm in the ^{1}H, ^{13}CO dimensions respectively. With 8 scans per increment and a relaxation delay of 6s, the total time was 3hours and 48minutes. After zero filling and apodization with a squared sine bell in the two dimensions, it was transformed as a matrix of 8k x 1k points. Processing was done with the Bruker Topspin software.

4) Data analysis

To measure the absolute ^{13}C incorporation at the Cα position, the HISQC-TOCSY spectra were run with different d1 delays (Fig. 2; Fig. S3). 1D spectra were extracted as the sum of the 1D traces covering all three peaks, to take into account the isotope shift of the ^{15}N frequency (Fig. 2). Peaks were integrated, and the integral of the central ($^{12}C\alpha$) peak was compared to the sum of the integrals of the ($^{13}C\alpha$) satellites. Alternatively, peaks were deconvoluted after manual peak picking as a sum of Gaussian peaks with the dcon algorithm as implemented in Topspin 3.0 (Figure S3-2), and the integrals of the satellites were compared to the sum of the integrals over all isotopomers. Both methods proved fully consistent with one another. The values given in the main text correspond to the averages and standard deviation over 4 independent experiments, with d1=1s, 2s and 2x4s.

To measure the ^{13}C incorporation at the CO position for those amino acids that have a $^{13}C\alpha$ nucleus, we extracted the planes from the 3D HNCA experiment at the ^{15}N value of the amino acid under investigation, and obtained 1D traces by summing the columns over the full width of the peak. 1D traces from the 2D planes were extracted in a similar manner, by summing the columns over the full width of the cross peak. Traces were phase and baseline corrected before fitting.

Quantification of the cumulated isotopomers observed in the HNCA spectra was done by fitting, assuming that the measured spectra are the linear sum of the individual isotopomer spectra. The theoretical spectrum of each isotopomer was modelled as a mixed Lorentzian-Gaussian line shape, given by:

$$F(x) = a \cdot L(x) + (1 - a) \cdot G(x)$$

where

$$L(x) = \frac{h}{1 + \left(\frac{x - X \pm J + c}{w}\right)^2}$$

and

$$G(x) = \mathrm{h} \cdot e^{-\log 2 \cdot \left(\frac{x - X \pm J + c}{w}\right)^2}$$

where $F(x)$ is the simulated signal amplitude at the chemical shift *x*, *X* is the chemical shift of the peak considered, *a* is the proportion of Lorentzian, *w* is the resolution, *h* is the isotopomer amplitude, and *c* is a slight chemical shift caused by neighbor ^{13}C nuclei.

All the parameters (chemical shifts, coupling constants, proportion of Lorentzian and Gaussian line shape, resolution, shifts in chemical shifts caused by neighbor ^{13}C nuclei) and the amplitude of each isotopomer was estimated using the nnls algorithm of R. Suitable starting values for these parameters were retrieved from the NMR spectra of standards or from the literature[5].

The values given in the main text correspond to the averages and standard deviation over 3 independent 2D experiments with d1=1s, 2s, and 4s.

The values extracted from the 3D experiment with d1=1s are given in the Table S1.

Residue	^{13}CO ($^{13}C\alpha$) incorporation (%)
Leu	49.8
Ala	50.5
Lys	50.1
Val	50.9
Ile	50.2
Phe	50.5
Glu	50.4
Ser	49.6
Thr	50.4
Gly	50.9

Table S1 Values for the ^{13}CO ($^{13}C\alpha$) incorporation as assessed from the 3D HNCA experiment. The theoretical value for this standard PT sample is 50%. As this experiment was run only once, we do not give any error bars on the numbers. Values in the main text are the average over different independent experiments run as a 2D H(N)CA plane.

To measure the ^{13}C incorporation at the Cα position for those amino acids that have a ^{13}CO nucleus ($^{13}C\alpha$ (^{13}CO)), we fitted the cross peaks in the 2D Hα-CO experiment by the Gaussian deconvolution algorithm as implemented in the Bruker Topspin2.0 software. Integration of the

combined $^{13}C\alpha$ linked $^{1}H\alpha$ peaks and comparison to the integral of the full $^{1}H\alpha$ peak gives the fractional ^{13}C incorporation for the $C\alpha$ position. Because proton magnetization in this experiment corresponds to the $H\alpha$ term, the contribution of the $^{13}C\alpha$ –$^{1}H\alpha$ dipolar interaction has to be taken into account, leading firstly to the requirement of a relaxation delay of at least 6s. The same differential relaxation of the $^{13}C\alpha$ linked $H\alpha$ protons compared to the $^{12}C\alpha$ linked $H\alpha$ protons leads however to an additional confounding factor that cannot be corrected by lengthening the relaxation delay. Indeed, the proton magnetization evolves in the xy plane during the INEPT transfer periods when $^{1}H\alpha$ magnetization evolves in a ^{13}CO anti-phase term, and equally in the inverse transfer. These transfer periods are lengthy due to the small coupling constant between $^{1}H\alpha$ and ^{13}CO spins, and one should correct for their differential relaxation properties during a total period of $4*\Delta+2*\Delta3$ (Figure S5-4). Because we can expect short τ_c values for the individual amino acids even at low temperatures, the relevant T_2 transverse relaxation time can be approximated by the longitudinal T_1 relaxation time. We measured this latter value by incorporating a 180° proton pulse before the HA-CO sequence of Figure S5-4, and varying the delay between this 180° pulse and the first proton 90° pulse of the sequence. Spectra were recorded with delays equal to 1ms, 200ms, 400ms, 600ms, 800ms, 2s, 4s, were processed as before, and the intensities of the $^{13}C\alpha$ / $^{12}C\alpha$ linked $H\alpha$ protons were plotted as a function of recovery time. The resulting inversion-recovery curve gives a measure for the T_1 times of both the $^{13}C\alpha$ and $^{12}C\alpha$ linked $H\alpha$ protons for the different amino acids (Figure S7). In the Table S2 below, we give the average incorporation of $^{13}C\alpha$ in ^{13}CO labeled molecules as measured over 3 independent experiments. The Table contains the $^{13}C\alpha$ incorporation values before correction (defined as the ratio of the integral of the $^{13}C\alpha$ linked $H\alpha$ protons over that of all $H\alpha$ protons), the measured T_1 times and the resulting correction factor. The values in the

main text are the average and standard deviations of the $^{13}C\alpha$ incorporation over three independent experiments with d1=6s.

Residue	$^{13}C\alpha$ (^{13}CO) incorporation (%)	T_1 (Hα) (ms) $^{13}C\alpha/^{12}C\alpha$	Correction factor	Corrected $^{13}C\alpha$ (^{13}CO) incorporation (%)
Leu	44.4± 0.2	470/870	1.18	48.5 ± 0.2
Ala	47.3± 0.2	760/1400	1.11	49.8 ± 0.2
Lys	44.2± 0.2	410/890	1.25	49.8± 0.2
Met	49.4± 1.2	510/890	1.15	53.0±1.2
Arg	43.8± 0.2	380/850	1.28	50.0± 0.2
Val	44.5± 0.4	550/1020	1.15	48.1± 0.4
Ile	45.1± 0.6	500/880	1.16	48.7± 0.6
Glu	45.8± 0.5	450/970	1.22	50.3± 0.5
Thr	45.3± 0.8	520/1000	1.17	49.2± 0.8
Gly	46.8± 0.4	800/1120	1.06	48.3± 0.4

Table S2. The first column gives the ^{13}CO conditioned $^{13}C\alpha$ incorporation, defined as the integral of the $^{13}C\alpha$ linked Hα protons /sum of the integrals of $^{13}C\alpha$ and $^{12}C\alpha$ linked Hα protons. No correction factor for differential relaxation of both components is taken into

account. The second column gives the measured T_1 relaxation times for the $^{13}C\alpha$ and $^{12}C\alpha$ linked Hα protons. The 3rd column is the correction factor due to the differential relaxation of $^{13}C\alpha$ and $^{12}C\alpha$ linked Hα protons during the INEPT transfers of the Ha-CO pulse sequence. The final column gives the corrected $^{13}C\alpha$ incorporation.

5) Complete isotopomer determination

When making abstraction of the side chain carbons and only focusing on the Cα and CO positions, every amino acid can be represented by 4 isotopomers, depending on the ^{12}C or ^{13}C incorporation at these 2 positions. As their sum is equal to the total concentration of the amino acid, that we put here arbitrarily to 100%, this gives only three independent variables to be determined. The combined experiments in Figures 2, 3 and 4 give 3 independent measures that should be sufficient to determine the three variables. We demonstrate this here on a fictitious example that further sheds light on how the measures determine the variables that are the isotope concentrations.

HISQC-DIPSI	32% $^{13}C\alpha$	68% ^{12}C	Absolute value
H(N)CA	40% ^{13}CO / 60% ^{12}CO		Relative value ($^{13}C\alpha$)
hence	12.8% $^{13}C\alpha/^{13}CO$	19.2% $^{13}C\alpha/^{12}CO$	Absolute value
Hα-CO	30% $^{13}C\alpha/^{13}CO$	70% $^{12}C\alpha/^{13}CO$	Relative value (^{13}CO)
hence	12.8 x 70 /30 = 29.9% $^{12}C\alpha/^{13}CO$		Absolute value
hence	29.9 + 12.8 = 42.7% ^{13}CO		Absolute value
hence	100 – 42.7 = 57.3% ^{12}CO		Absolute value

hence 100 – 12.8 -19.2 -29.9 = 38.1% $^{12}C\alpha/^{12}CO$ Absolute value

In blue are indicated the absolute values of the different isotopomers.

6) Flux analysis as a function of G6PDH levels

A targeted ^{13}C-metabolic flux analysis experiment was designed to quantify fluxes through the glycolytic and pentose phosphate (PPP) pathways of *E. coli*. Experiments were carried out in *Escherichia coli* K-12 MG1655 and its derivative mutants (Pzwf1.1, Pzwf1.3, and Pzwf3) with gradual expression of the *zwf* gene encoding the glucose-6-phosphate dehydrogenase (G6PDH), which catalyzes the first step of the pentose phosphate pathway (PPP). Fluxes were estimated from the four isotopomers of the (Cα, CO) two-carbon block of leucine, which derive from the acetyl moiety of acetylCoA (AcCoA, as detailed below).

Cells were grown in M9 minimal medium (50 mL, baffled shake flask, 180 rpm, 37°C) containing 1,2-$^{13}C_2$-glucose and $^{15}NH_4^+$ as sole carbon and nitrogen sources, respectively, and the ^{13}C-incorporation into proteinogenic amino acids was measured using the HISQC-TOCSY, HNCA and HACO experiments. All experiments on a single sample, including the reference HISQC spectrum, were completed in 6 hours, leading to a total acquisition time of one day for the four samples. Results obtained for leucine isotopomers are given in Table S3. Since several carbon positions of different metabolites come from the same metabolic precursors, we checked the consistency between leucine measurements and redundant isotopic information (the four acetate isotopomers and the specific enrichment of Cβ of alanine). Differences were below 1.5%, indicating that the isotopic data are self-consistent.

Experiment	Isotopomer	Pzwf1.1	Pzwf1.3	WT	Pzwf3
HNCA	010xxx	0.013	0.032	0.072	0.078
	110xxx	0.520	0.514	0.516	0.514
	011xxx	0.007	0.017	0.040	0.055
	111xxx	0.461	0.437	0.372	0.352
HISQC-TOCSY	x0xxxx	0.543	0.551	0.564	0.565
	x1xxxx	0.457	0.449	0.436	0.435
HACO	10xxxx	0.059	0.034	0.063	0.080
	11xxxx	0.941	0.966	0.937	0.920

Table S3. Quantification results of leucine isotopomers obtained from the HNCA, HACO-DIPSY and HISQC-TOCSY experiments for the four *E. coli* strains. *0* denotes ^{12}C atoms at the corresponding carbon position, *1* denotes ^{13}C atoms, and *x* denotes either ^{12}C or ^{13}C atoms.

Estimation of the PPP and glycolytic fluxes was based on the absolute quantification of the four isotopomers for the (Cα, CO) two-carbon block of the isotopomers of leucine, which are given in Table S4.

Isotopomer	Pzwf1.1	Pzwf1.3	WT	Pzwf3
00xxxx	0.515	0.536	0.538	0.532
10xxxx	0.028	0.015	0.026	0.033
01xxxx	0.009	0.022	0.049	0.058
11xxxx	0.448	0.427	0.387	0.377

Table S4. Abundances of the four isotopomers of the (Cα, CO) two-carbon block of leucine measured for the four *E. coli* strains from data given in Table S3.

The (Cα, CO) two-carbon block of leucine derives from the acetyl moiety of AcCoA, as shown in Figure S9. When using [1,2-$^{13}C_2$]glucose as sole carbon source, glycolysis forms fully labeled and fully unlabeled AcCoA in the same proportions. In contrast, C_1-decarboxylation of glucose through the oxidative branch of the PPP produces 2-^{13}C-leucine, and carbon scrambling

caused by reversibility produces mainly unlabeled but also singly and fully labeled CO-Cα-leucine – at a lower abundance.

For all the strains, most of the CO-Cα block of leucine was unlabeled or fully labeled (representing 91-96% of the total pool). The low proportion of 1-^{13}C-leucine (below 3% for all strains) suggests that the reversible non-oxidative branch of the PPP contributes little to carbon scrambling of glycolytic intermediates. Hence, we assumed that 1,2-$^{13}C_2$-leucine mostly derive from direct glycolytic flux without going through PPP. The fraction of AcCoA derived from glycolysis was thus estimated using the following equation:

$$Glycolysis = 2 \times Leu_{11xxxx}$$

and the fraction of acetylcoA derived from the PPP was estimated to be:

$$PPP = 2 \times (0.5 - Leu_{11xxxx})$$

The relative glycolytic and PPP fluxes measured in the four strains (Table S5) are in excellent agreement with previous results,[6] but are superior in terms of precision and reduced acquisition time.

		This study		Heux et al., 2014	
Strain	G6PDH activity	Glycolysis (% glc uptake)	PPP (% glc uptake)	Glycolysis (% glc uptake)	PPP (% glc uptake)
Pzwf1.1	3.1±0.3	90±2	10±2	95±15	5±15
Pzwf1.3	11±1	85±2	15±2	94±16	6±16
WT	190±4	77±2	23±2	72±18	28±18
Pzwf3	1586±12	75±2	25±2	69±20	31±20

Table S5. G6PDH activity and metabolic fluxes through the glycolytic and pentose phosphate pathways measured in the four *E. coli* strains. Fluxes are expressed relatively to the glucose uptake rate.

Isotopic data from a single amino acid were exploited here for targeted ^{13}C-metabolic flux analysis. The proposed NMR experiments provide access to the complete isotopomer distribution of the CO-Cα block of many other amino acids (as well as partial information on the Cβ labeling). Of course, this information can be used in the context of more complete ^{13}C-metabolic flux analyses via detailed modelling approaches.

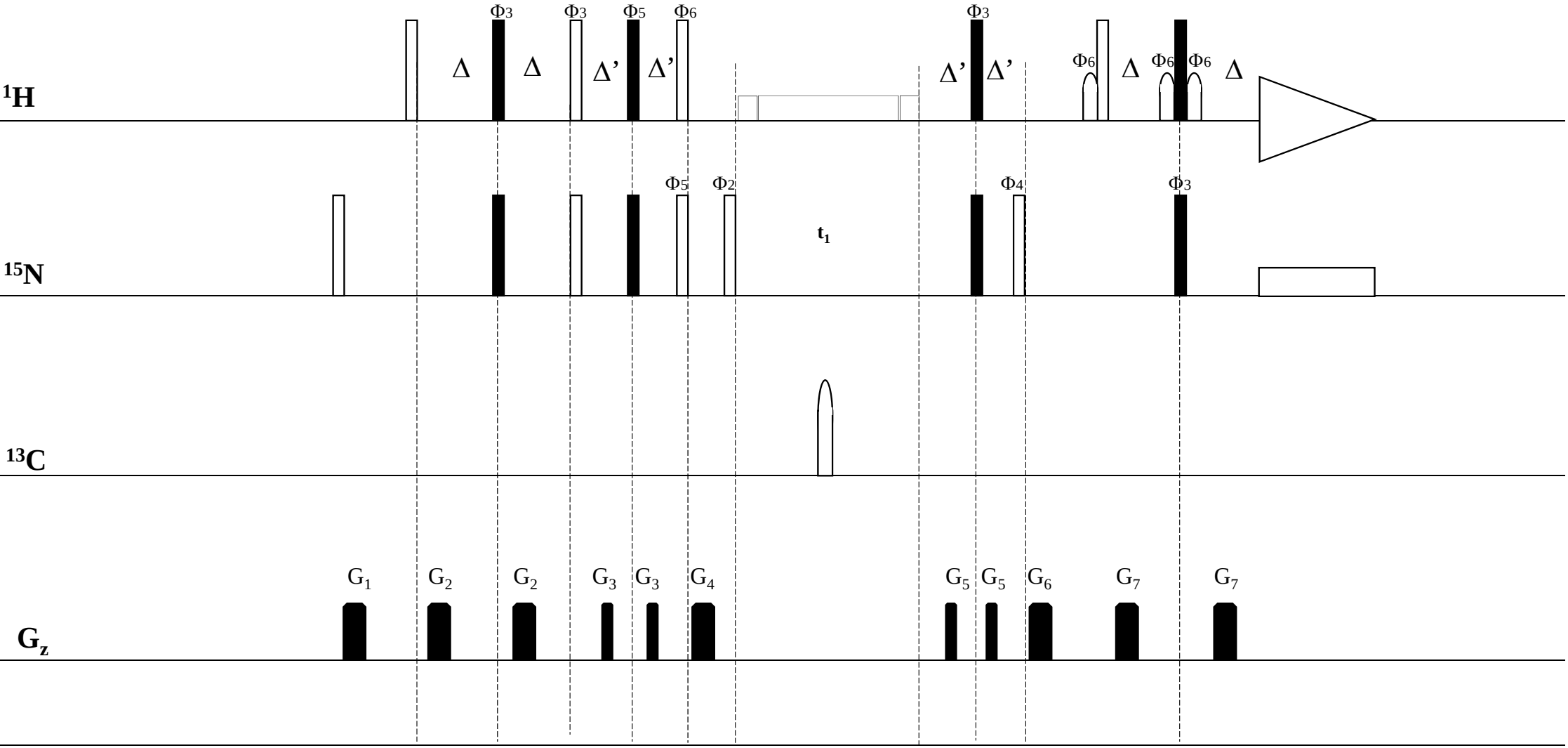

Figure S1 Pulse sequence of the ^{1}H, ^{15}N HISQC experiment.

Hard 90° or 180° pulses are indicated by open or filled rectangles. Phases are x unless otherwise indicated.
Φ2= y –y; Φ3 = y y –y –y; Φ4 = x x xx –x –x –x –x; Φ5 = y; Φ6 = -x; Acquisition phase = x –x –x x –x x x –x

Gradients are applied as smoothed sine waves, with length of 1ms for all except for G3 and G5 where the duration is limited to 500µs. Gradient strengths are 53% (G1), 47% (G2), 89% (G3), 31% (G4), 83% (G5), 43% (G6) and 77% (G7) of the maximal gradient strength.

During the t_1 evolution, Waltz16 proton decoupling isapplied to prevent the evolution of H_zN_{xy} terms that would suffer from rapid water exchange.

Water flip back pulses are applied as rectangular pulses with 1ms duration.
Carbon coupling during t_1 is refocused by a adiabatic 180° pulse centered at 100ppm.

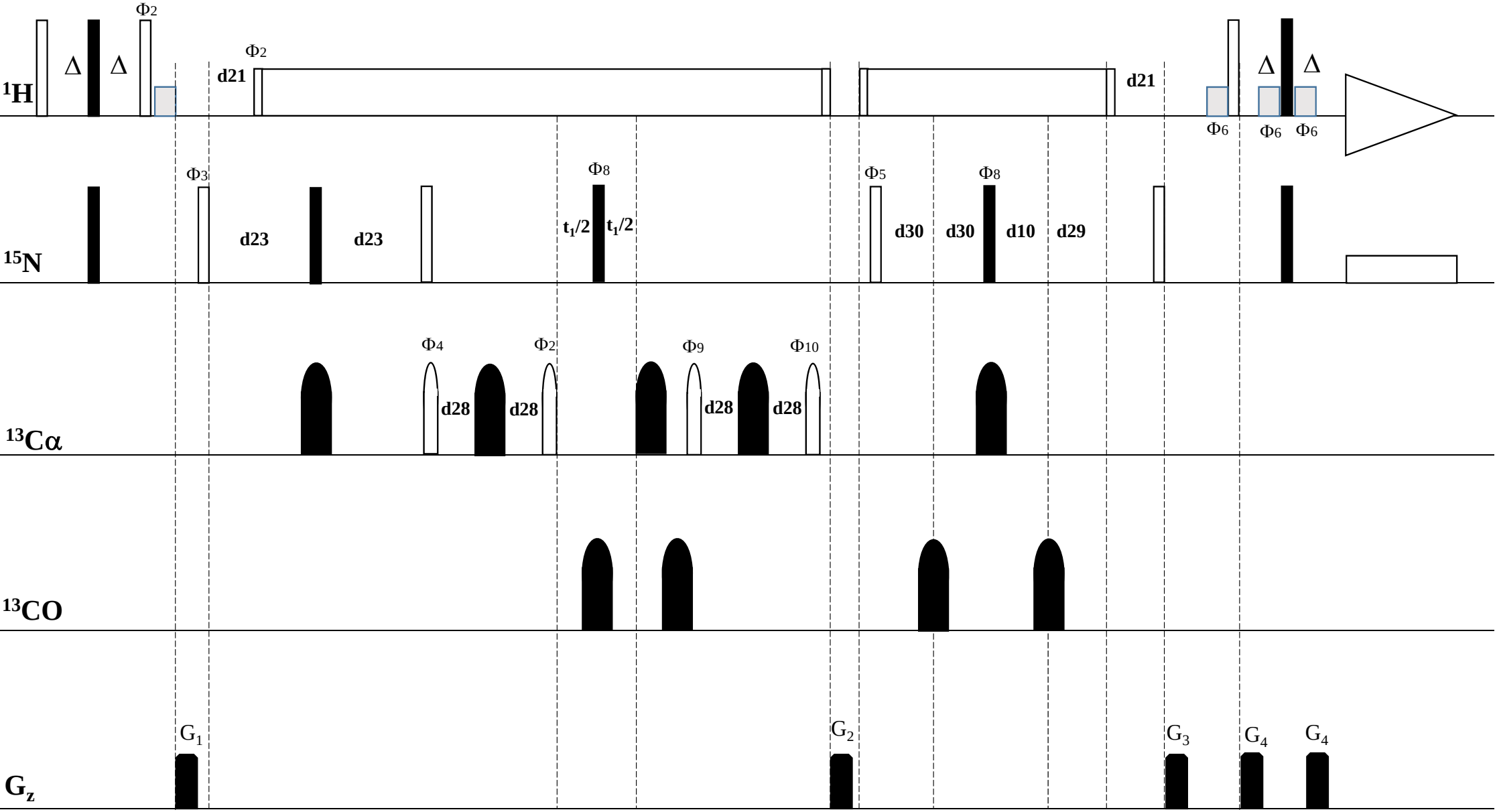

Figure S2-1 Pulse sequence of the HNCACB experiment adapted for free amino acids

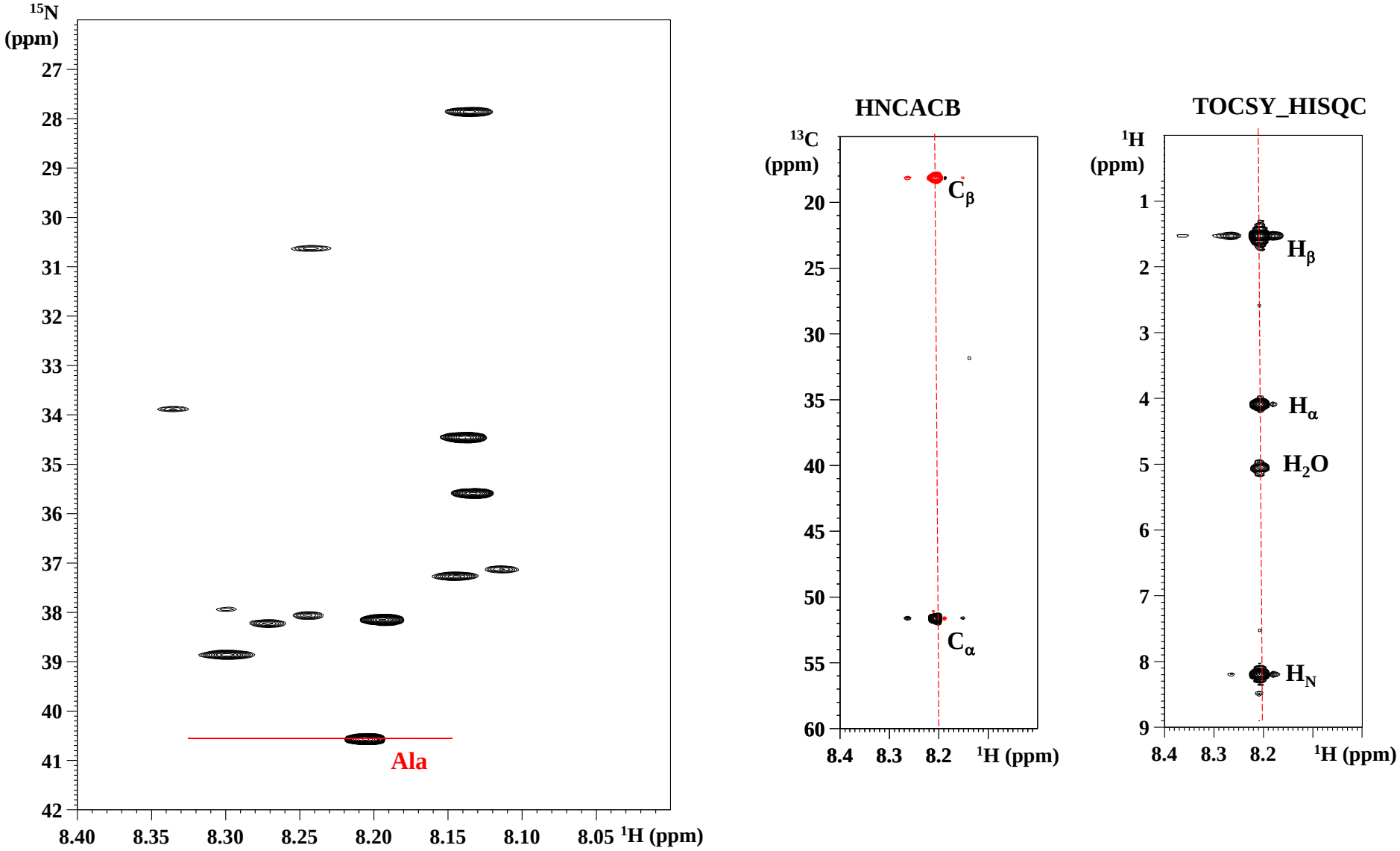

Figure S2-2

Strips extracted from the HNCACB and TOCSY-HISQC 3D experiments for the assignment of the different resonances in the hydrolyzed U-^{13}C/^{15}N algal extract.

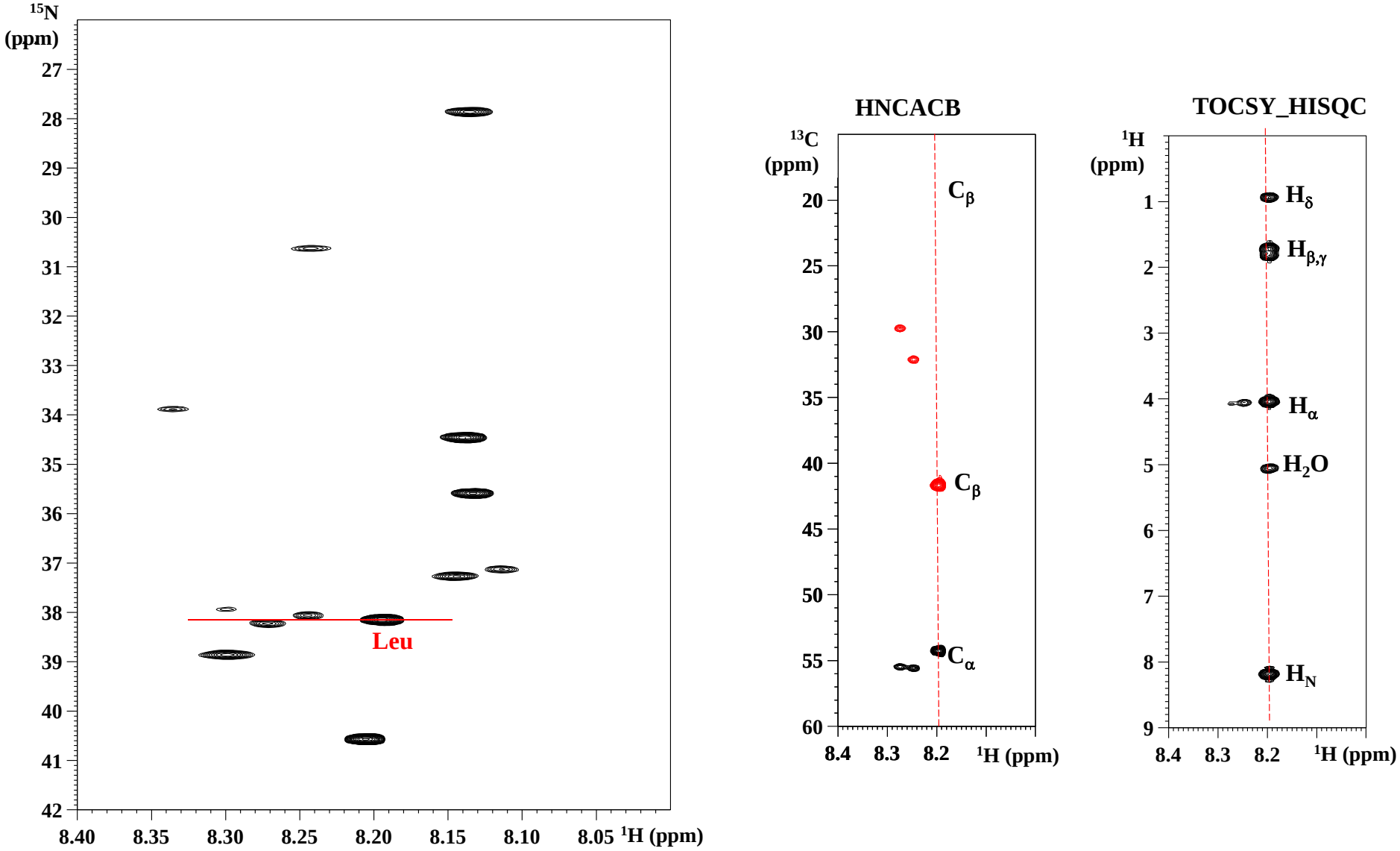

Figure S2-3

Strips extracted fromthe HNCACB and TOCSY-HISQC 3D experiments for the assignment of the different resonances in the hydrolyzed U-13C/15N algal extract.

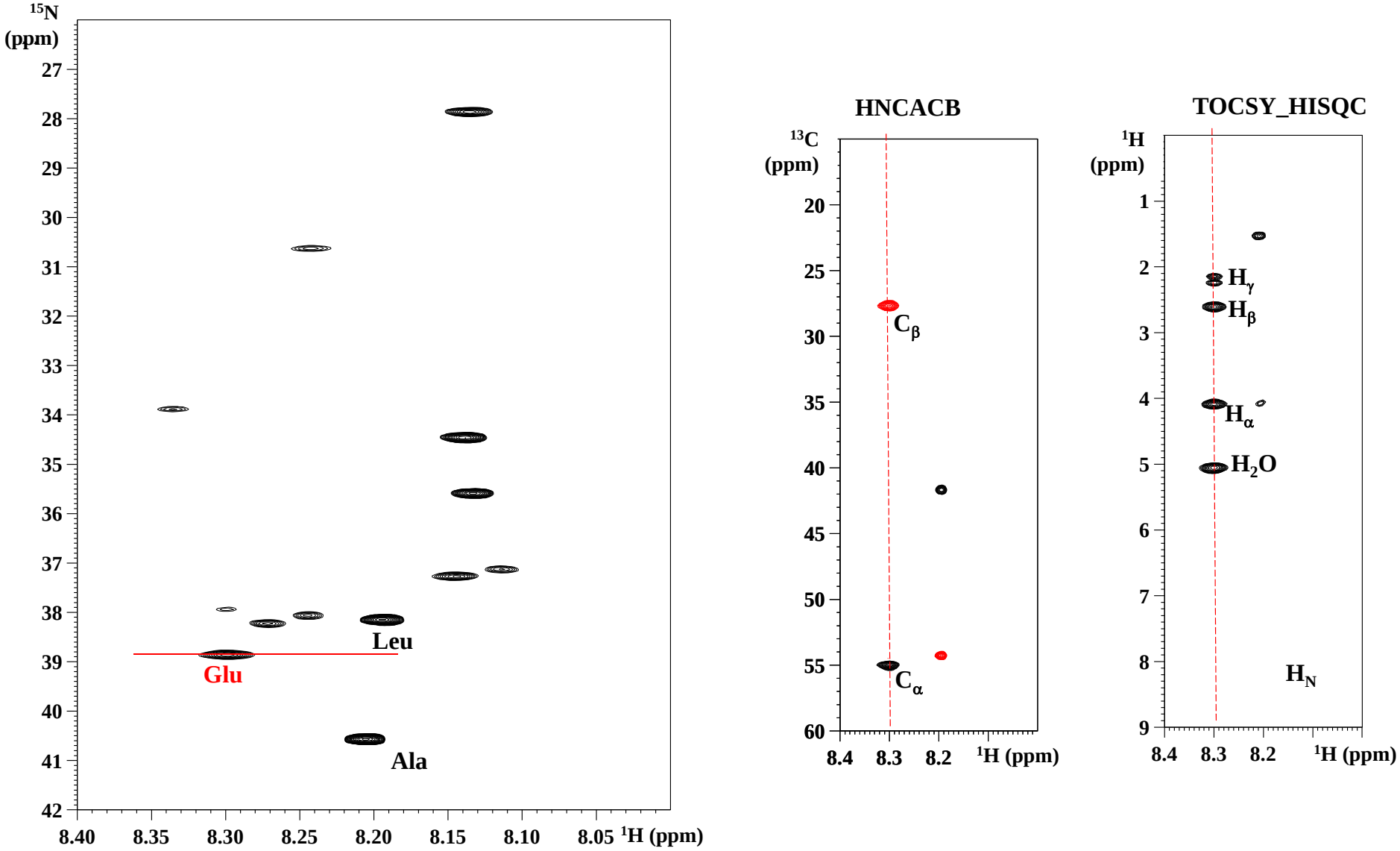

Figure S2-4

Strips extracted fromthe HNCACB and TOCSY-HISQC 3D experiments for the assignment of the different resonances in the hydrolyzed U-13C/15N algal extract.

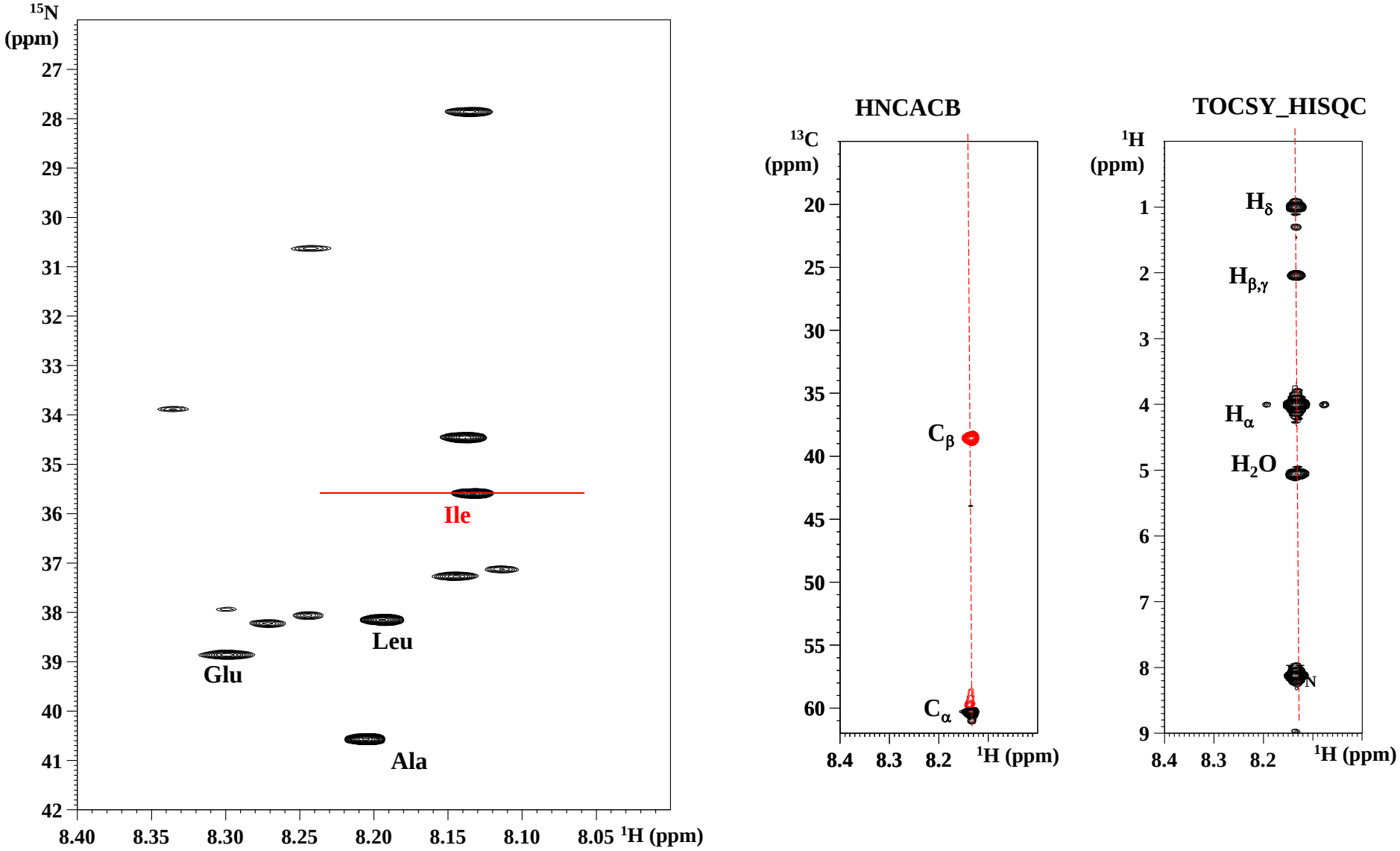

Figure S2-5

Strips extracted fromthe HNCACB and TOCSY-HISQC 3D experiments for the assignment of the different resonances in the hydrolyzed U-13C/15N algal extract.

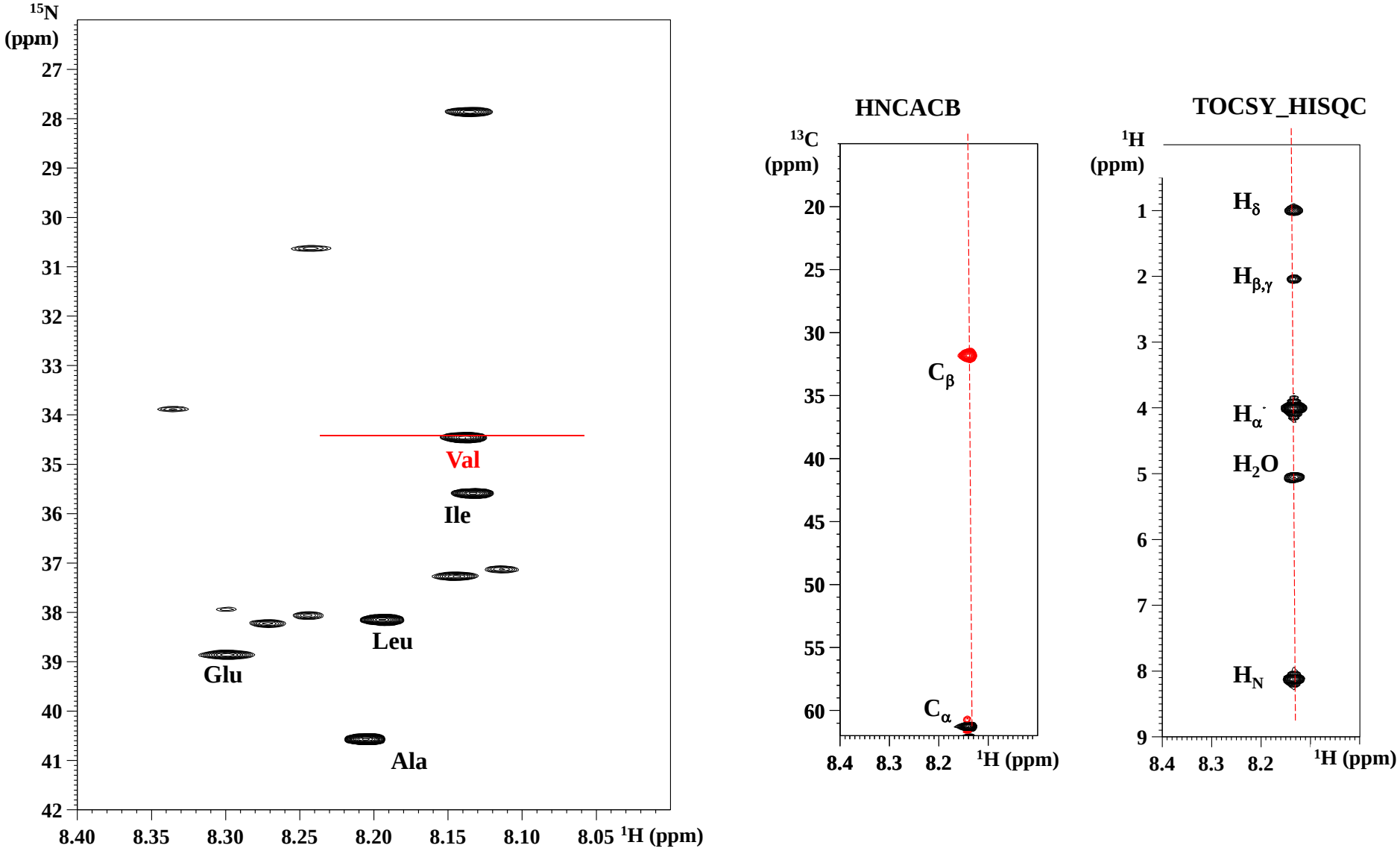

Figure S2-6

Strips extracted fromthe HNCACB and TOCSY-HISQC 3D experiments for the assignment of the different resonances in the hydrolyzed U-13C/15N algal extract.

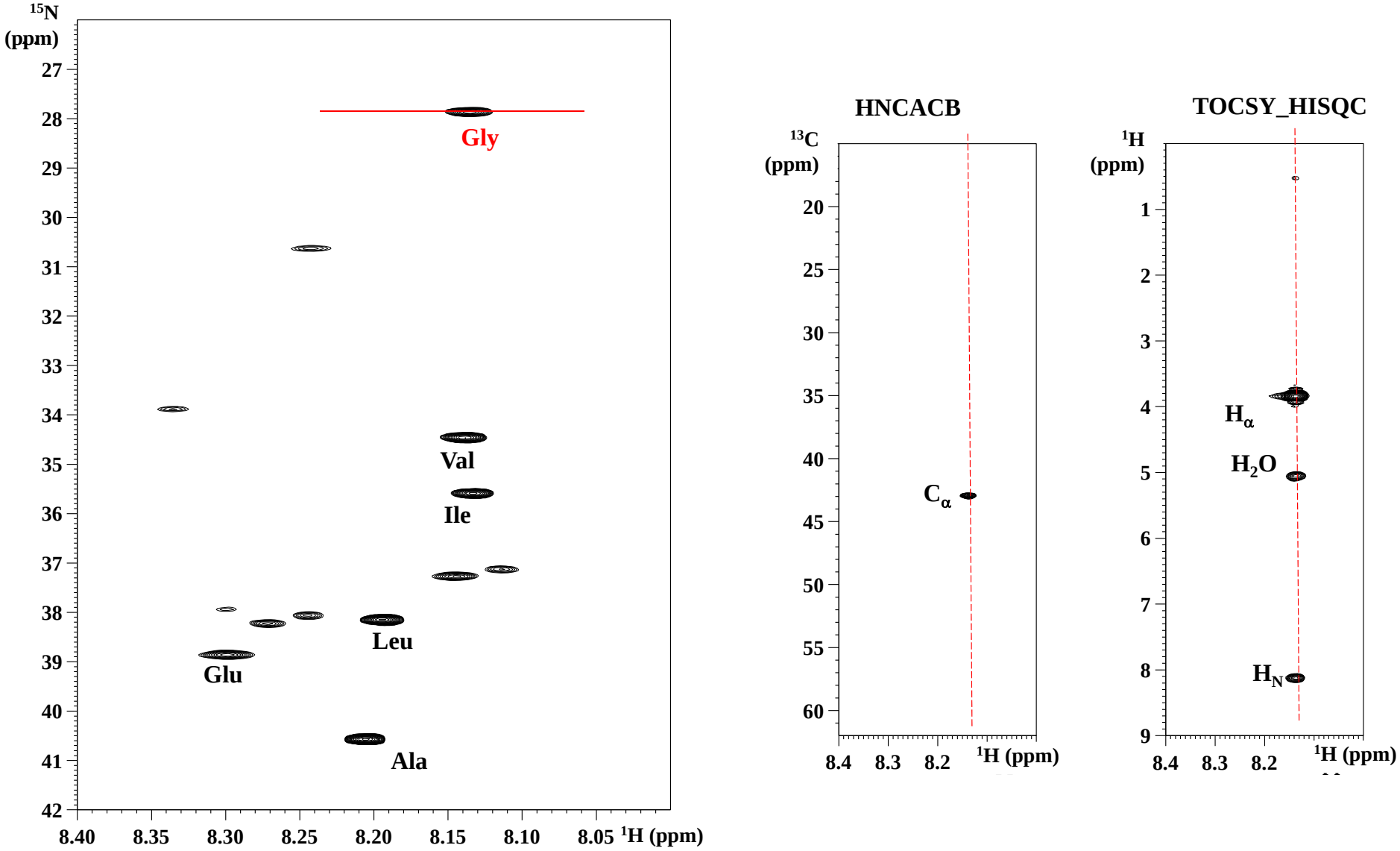

Figure S2-7

Strips extracted fromthe HNCACB and TOCSY-HISQC 3D experiments for the assignment of the different resonances in the hydrolyzed U-13C/15N algal extract.

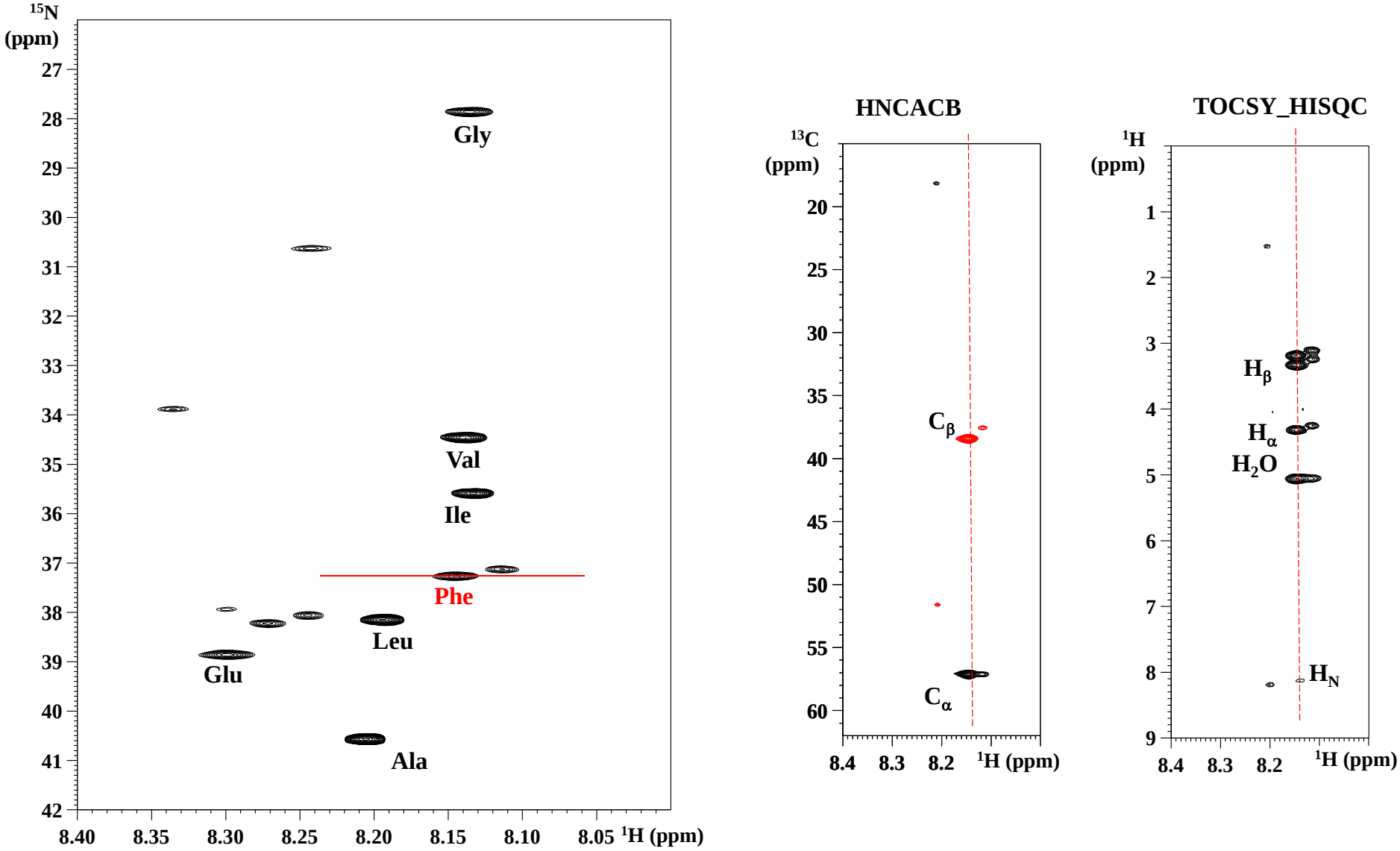

Figure S2-8

Strips extracted fromthe HNCACB and TOCSY-HISQC 3D experiments for the assignment of the different resonances in the hydrolyzed U-13C/15N algal extract.

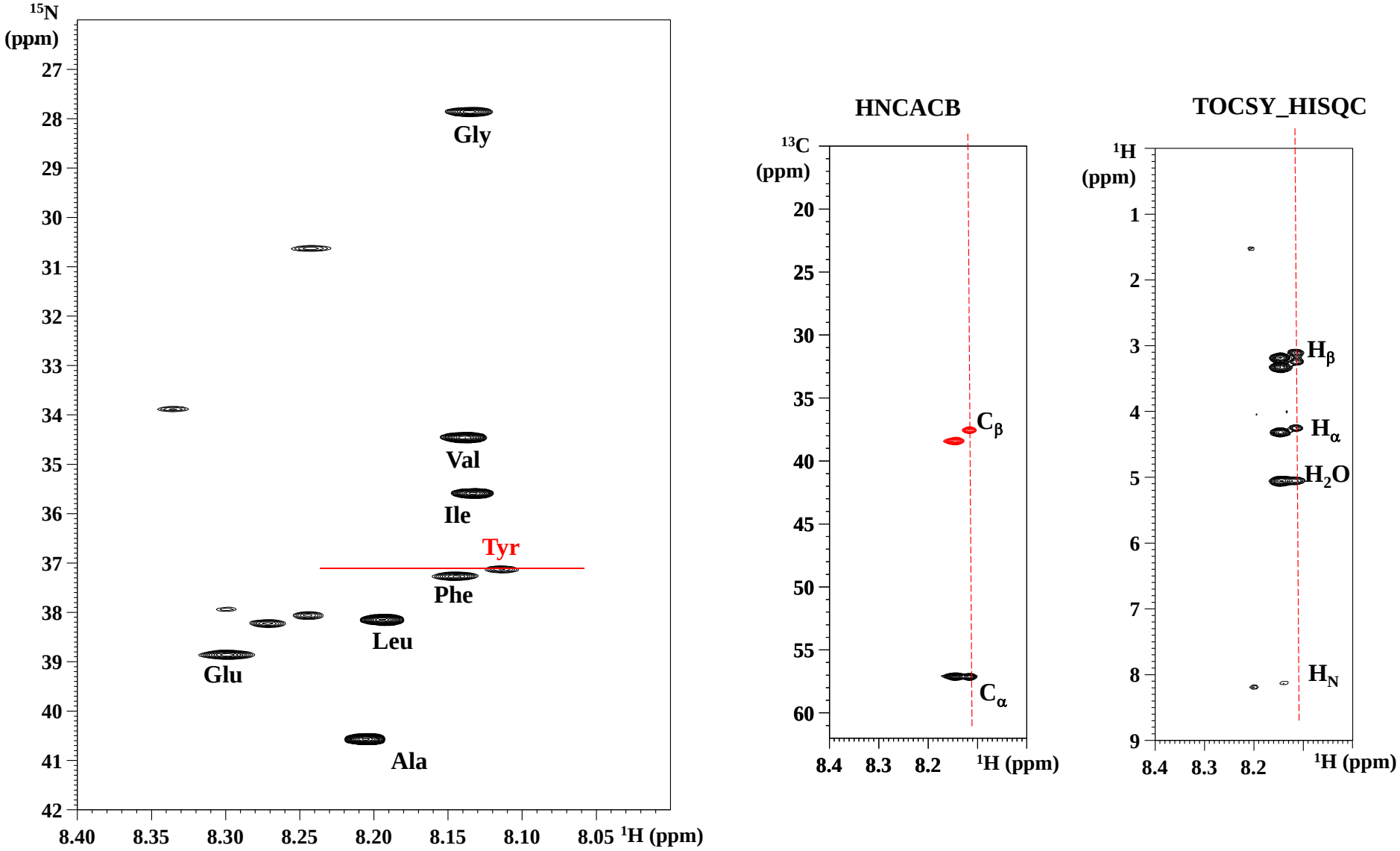

Figure S2-9

Strips extracted fromthe HNCACB and TOCSY-HISQC 3D experiments for the assignment of the different resonances in the hydrolyzed U-13C/15N algal extract.

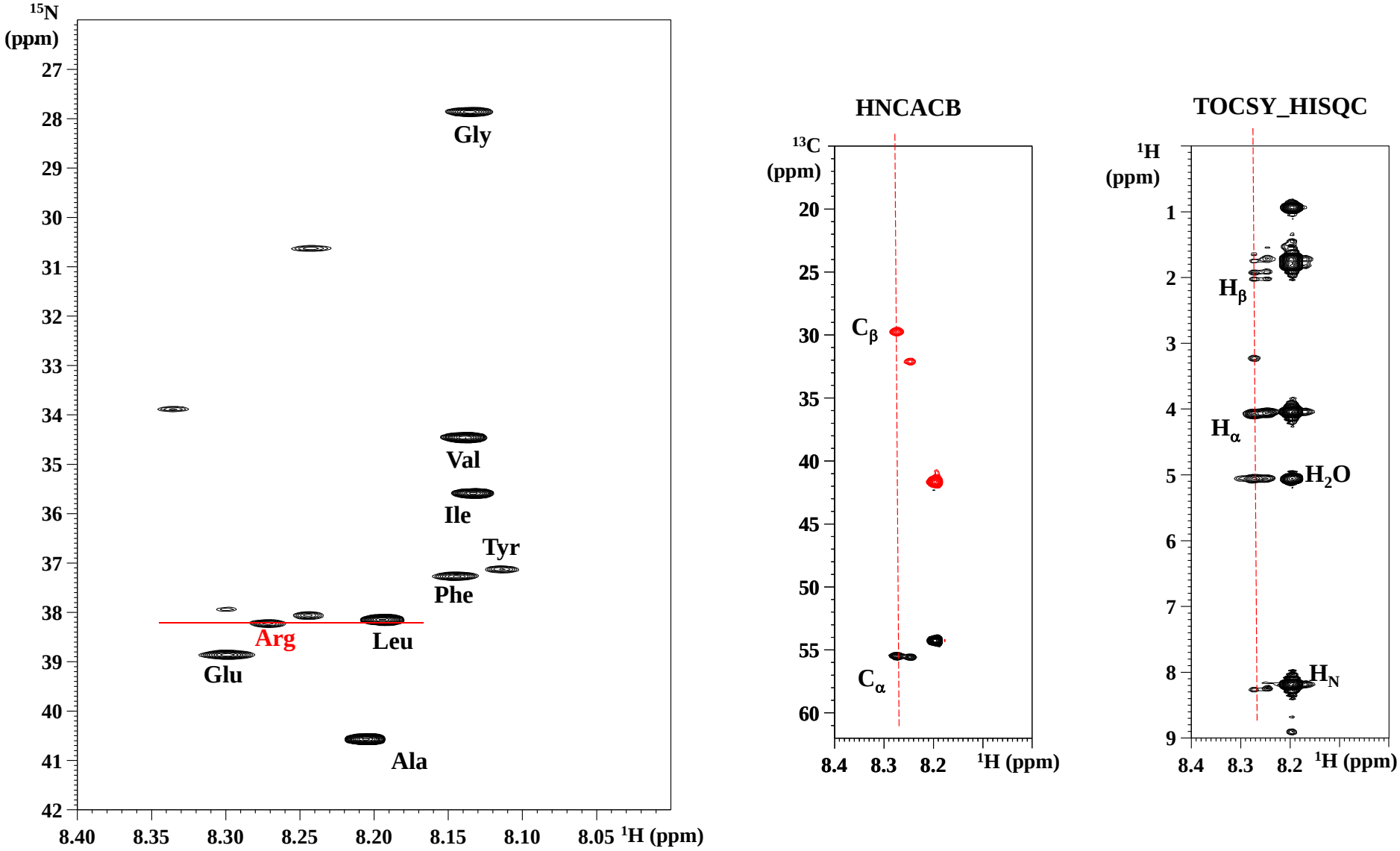

Figure S2-10
Strips extracted fromthe HNCACB and TOCSY-HISQC 3D experiments for the assignment of the different resonances in the hydrolyzed U-13C/15N algal extract.

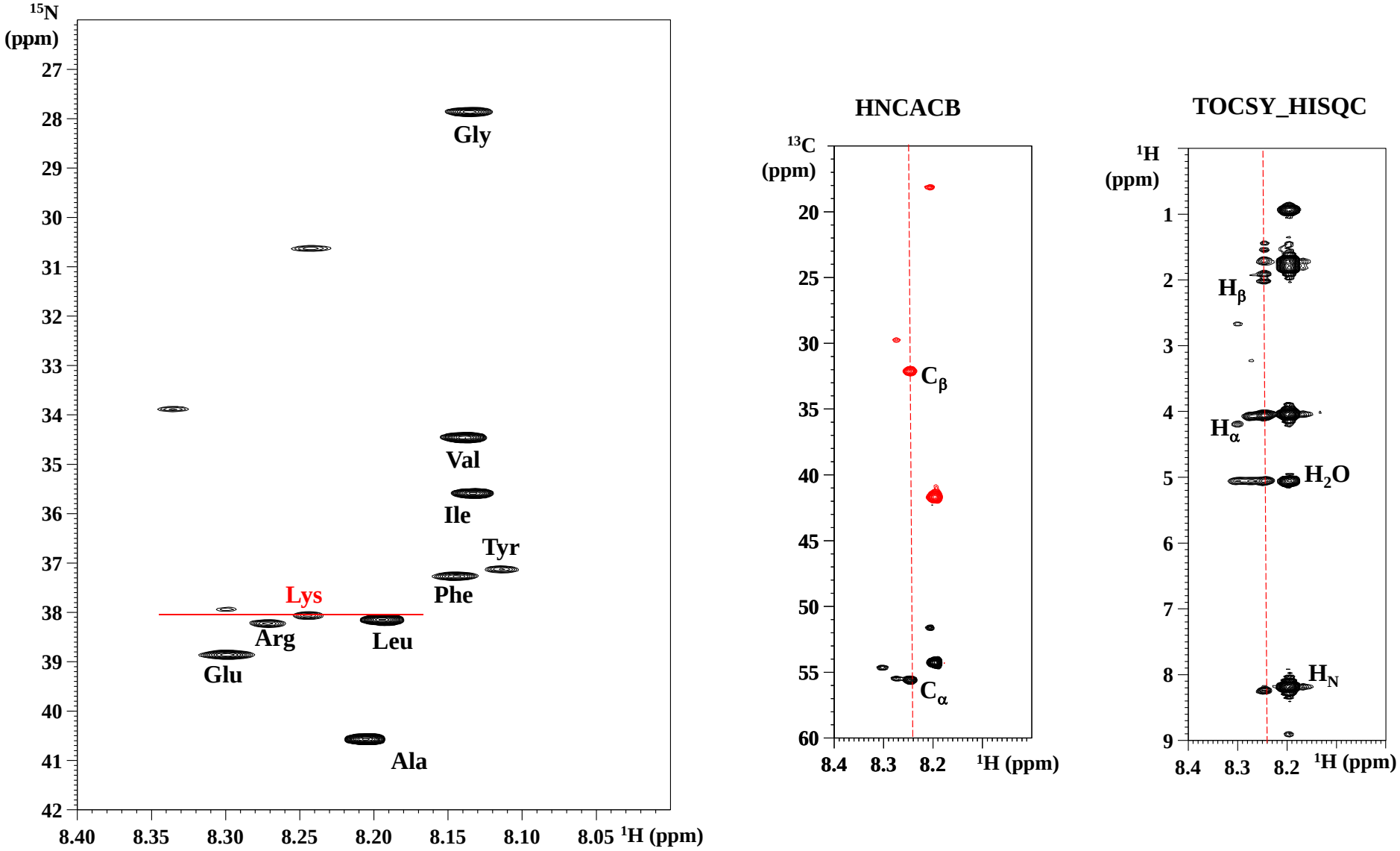

Figure S2-11

Strips extracted fromthe HNCACB and TOCSY-HISQC 3D experiments for the assignment of the different resonances in the hydrolyzed U-13C/15N algal extract.

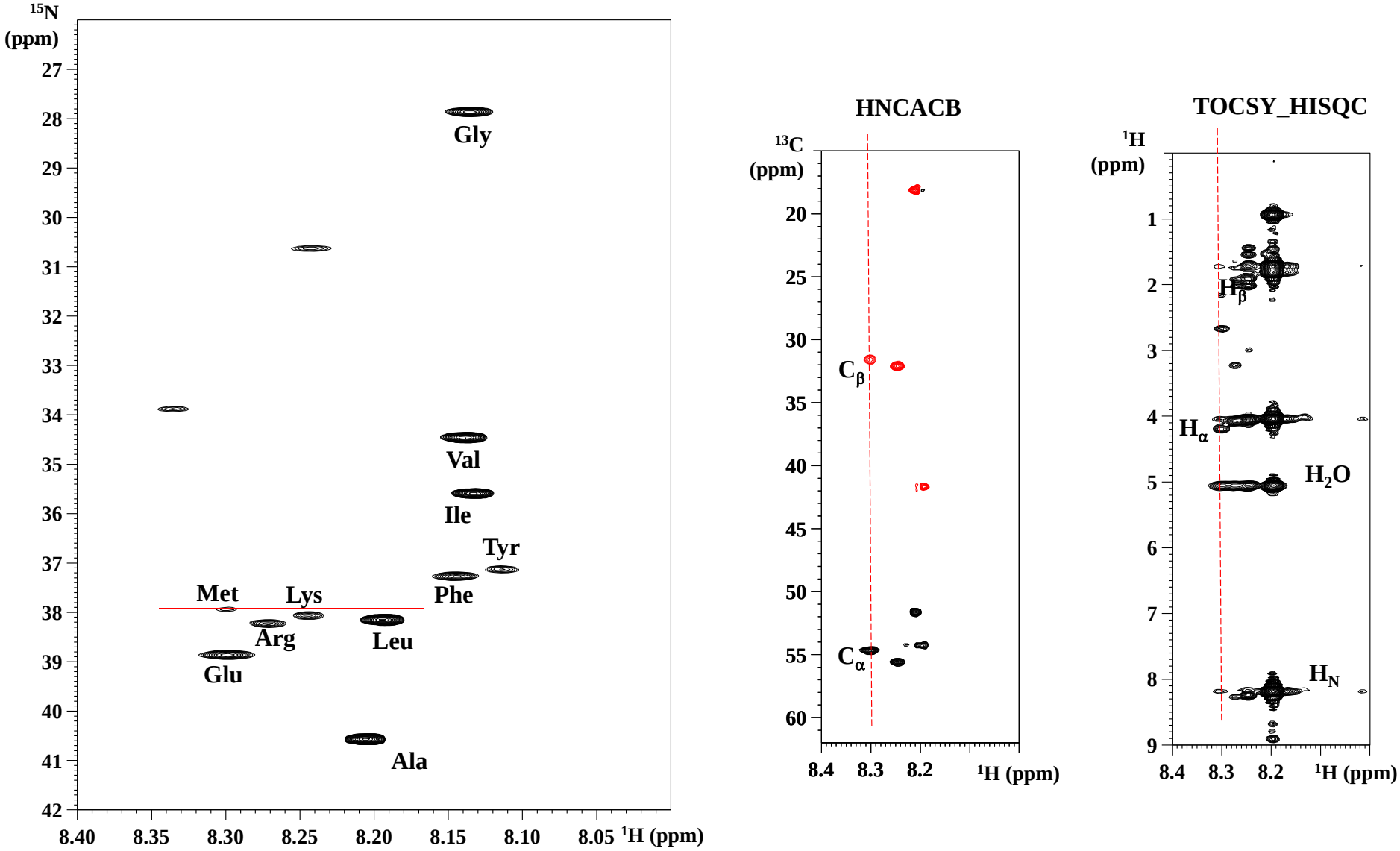

Figure S2-12
Strips extracted fromthe HNCACB and TOCSY-HISQC 3D experiments for the assignment of the different resonances in the hydrolyzed U-13C/15N algal extract.

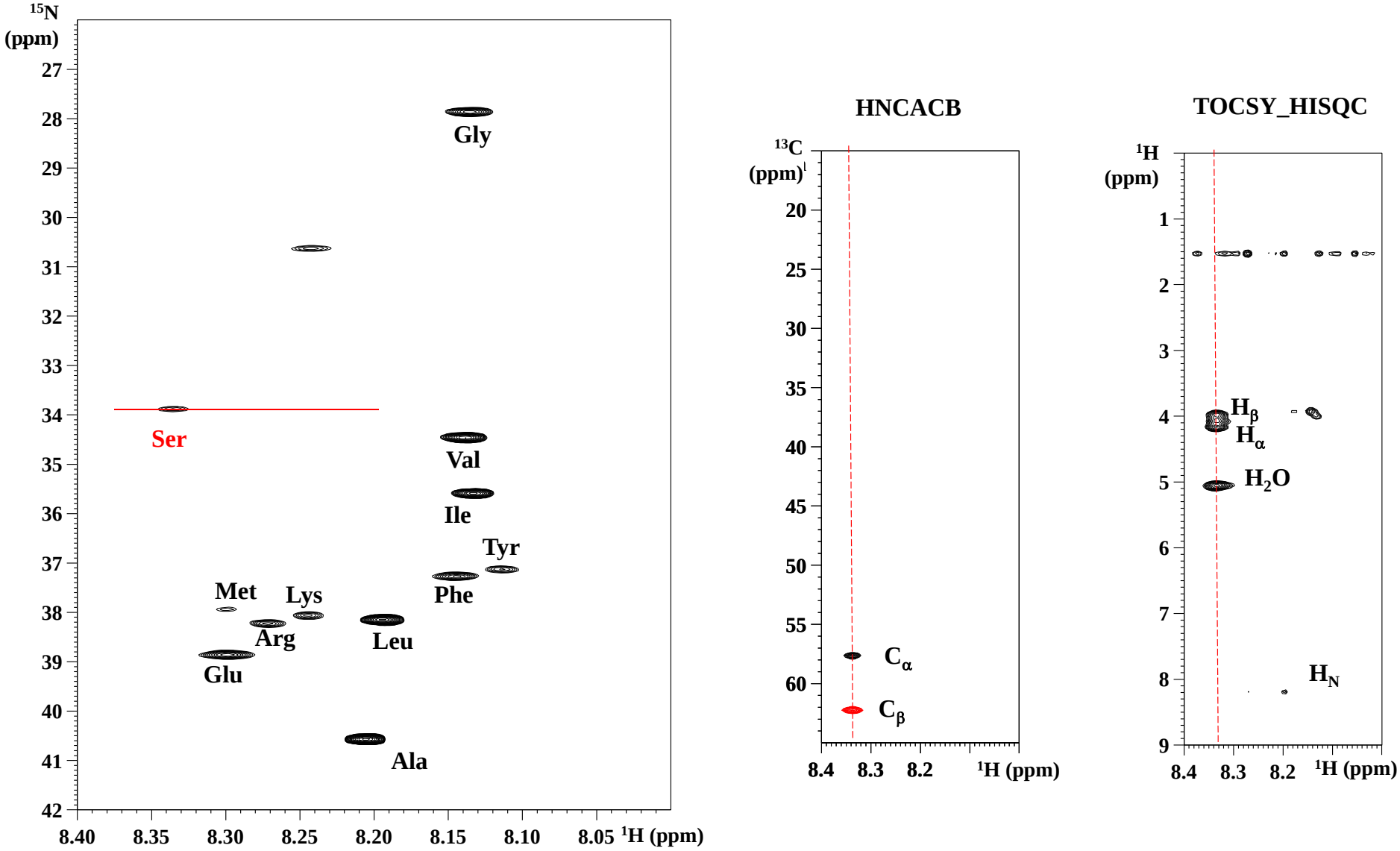

Figure S2-13
Strips extracted fromthe HNCACB and TOCSY-HISQC 3D experiments for the assignment of the different resonances in the hydrolyzed U-13C/15N algal extract.

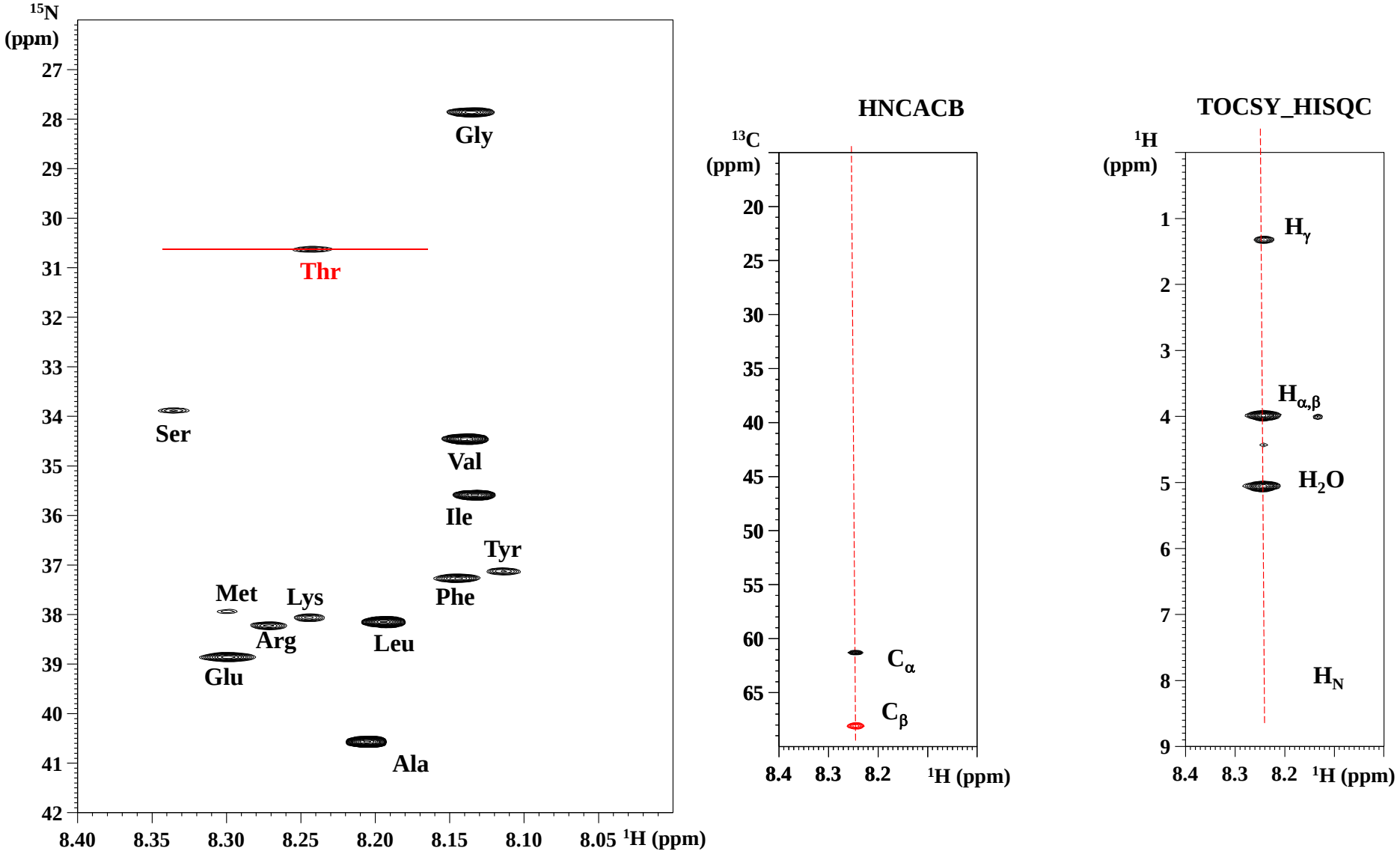

Figure S2-14
Strips extracted fromthe HNCACB and TOCSY-HISQC 3D experiments for the assignment of the different resonances in the hydrolyzed U-13C/15N algal extract.

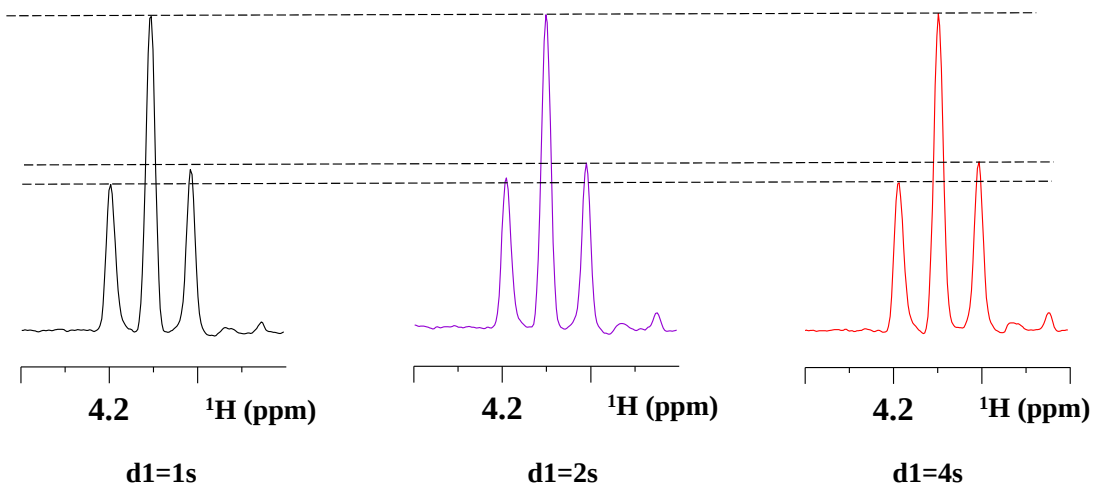

Figure S3-1

Traces through the Ala Hα-N resonance of the HISQC-TOCSY experiment run with a relaxation delay of 1, 2 or 4s. All spectra were acquired and processed identically.

Relative intensities of the $^{12}C\alpha/^{13}C\alpha$ linked Hα protons are identical within experimental error.

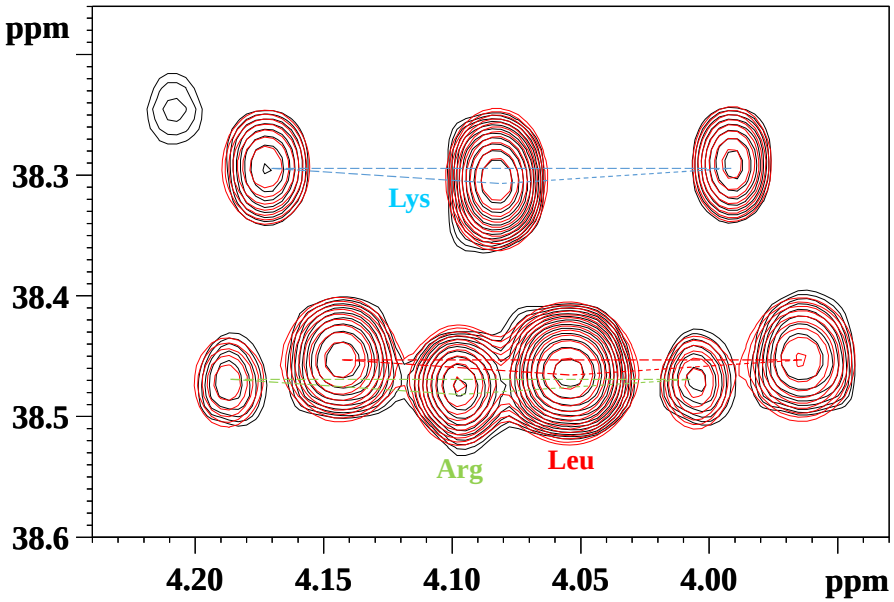

	$^{13}C\alpha$	$^{12}C\alpha$	$^{13}C\alpha$
Leu	**70.0**	**137.4**	**64.1**
Lys	**45.6**	**87.1**	**42.4**
Arg	**25.9**	**57.3**	**26.4**

Figure S3-2
Deconvolution of the Hα-N resonances of Leu, Arg and Lys in the HISQC-TOCSY experiment with a relaxation delay of 1s. The experimental data are in black, whereas the deconvoluted data set is in red.
Relative intensities of the $^{12}C\alpha/^{13}C\alpha$ linked Hα protons can be determined from the fitted integrals.

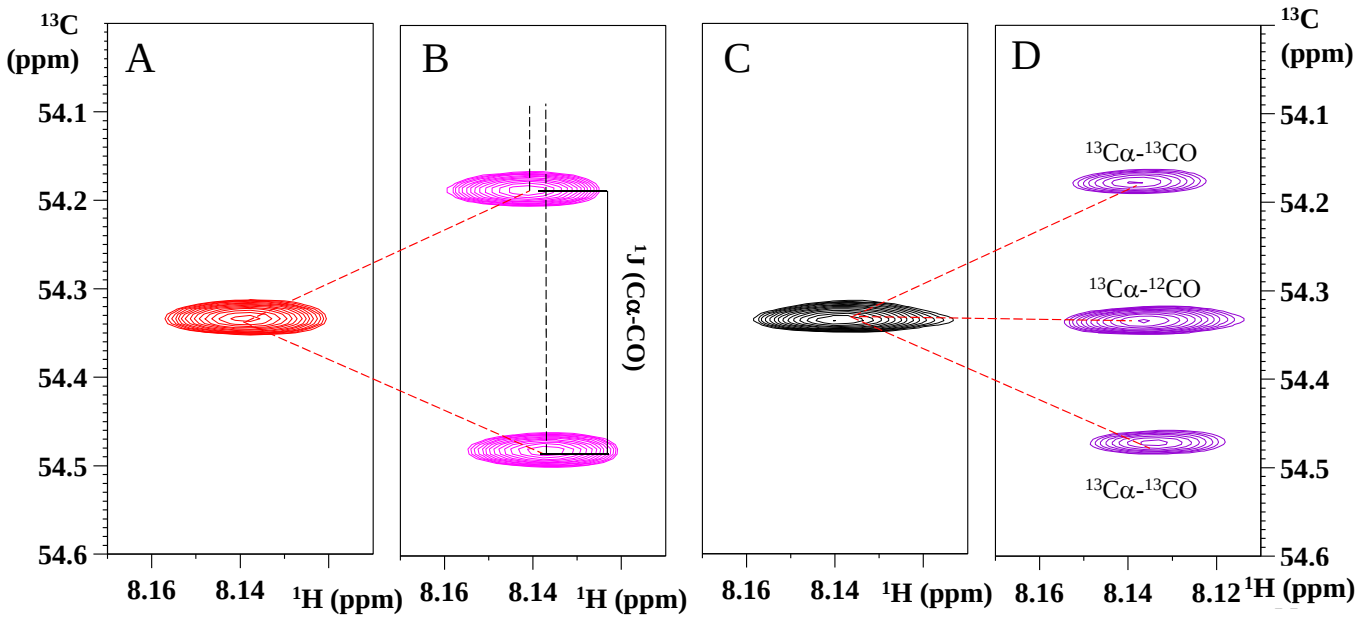

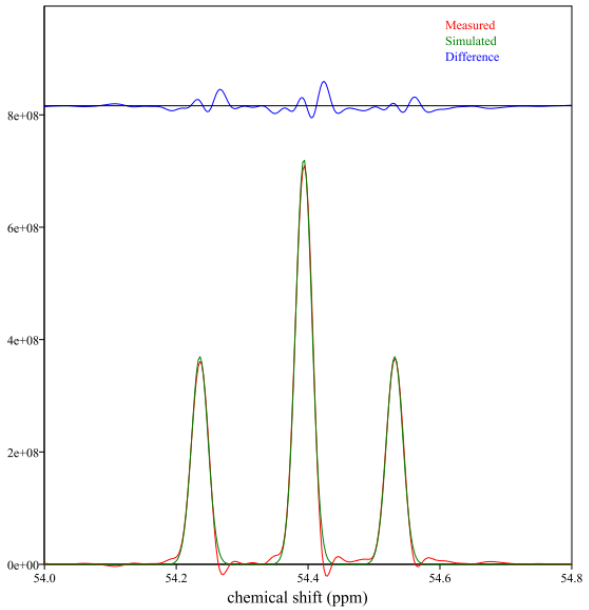

Figure S4-1

Zooms of the H(N)CA planes representing the **Gly** Cα resonance in the U-^{13}C (A,B) or PT-^{13}C (C,D) samples with (A,C) or without (B,D) ^{13}CO decoupling during the ^{13}Cα evolution.

The ratio of (^{13}Cα) ^{12}CO/(^{13}Cα) ^{13}CO can be directly measured from the integrals of the central line compared to the satellites.
From the coupling pattern in D, the ratio of (^{13}Cα) ^{12}CO/(^{13}Cα) ^{13}CO can be determined. The experimental projection and fitted signal are shown on the right.

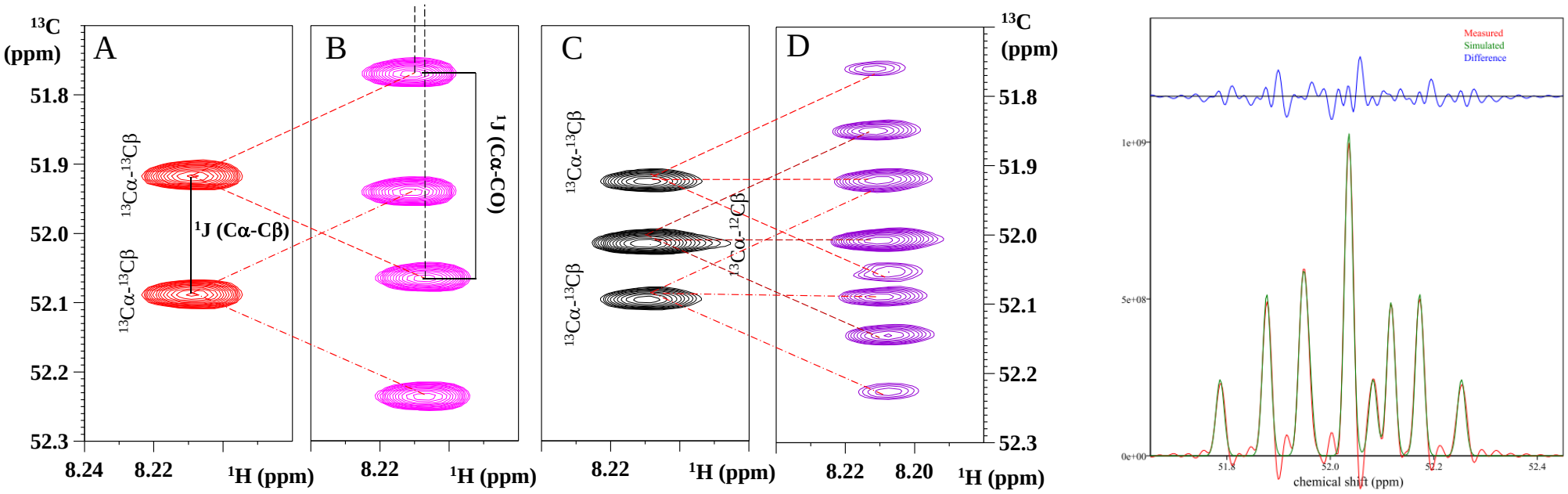

Figure S4-1

Zooms of the H(N)CA planes representing the **Ala** Cα resonance in the U-^{13}C (A,B) or PT-^{13}C (C,D) samples with (A,C) or without (B,D) ^{13}CO decoupling during the ^{13}Cα evolution.

The ^{13}Cα-^{13}Cβ coupling is active in all spectra when the Cβ position is labelled, and is only absent when the nucleus at the Cβ position is a ^{12}C isotope. From the coupling pattern in D, the ratio of (^{13}Cα) ^{12}CO/(^{13}Cα) ^{13}CO can be determined. The experimental projection and fitted signal are shown on the right.

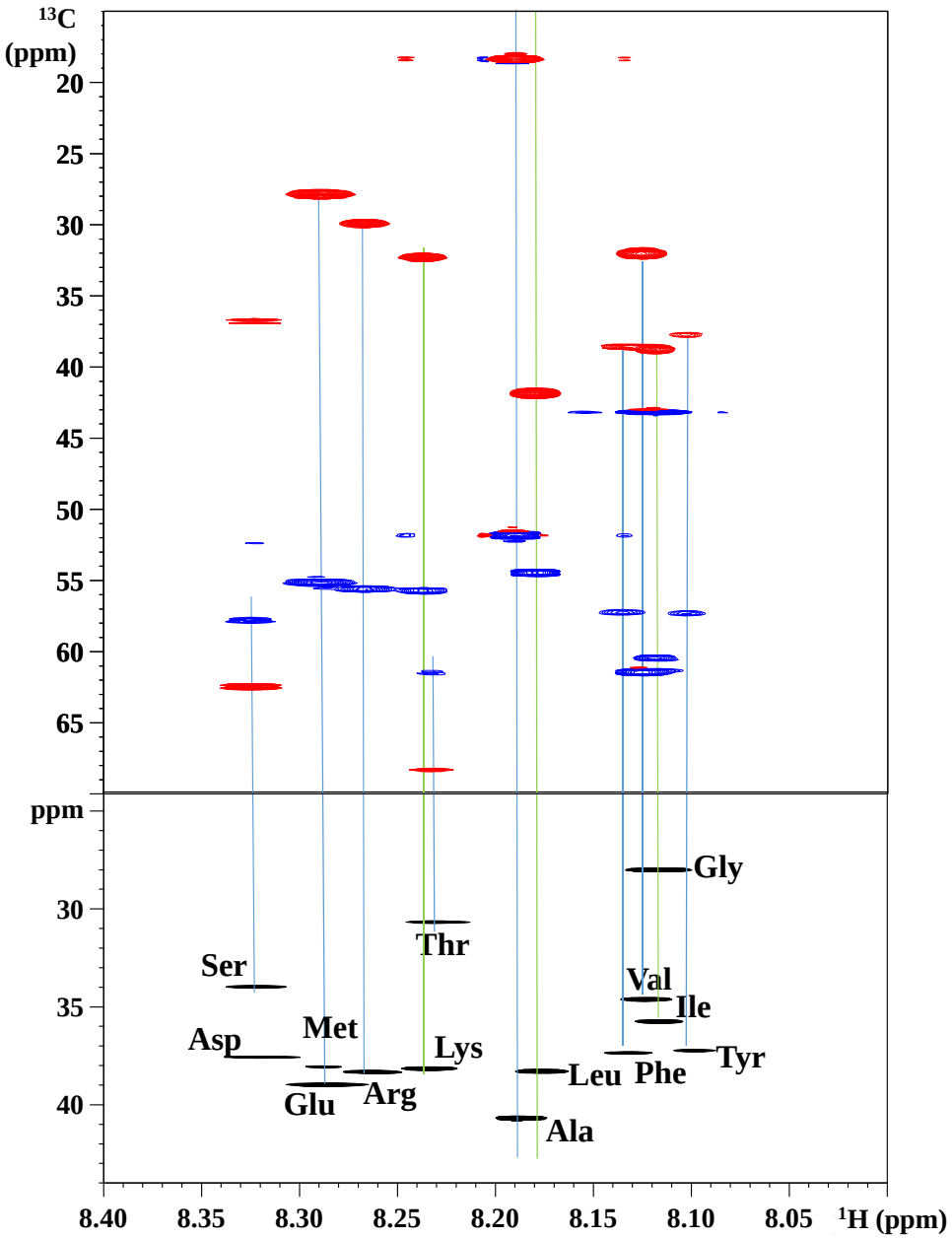

Figure S5-1 Plane from the HNCACB spectrum of the U-^{13}C/^{15}Nlabeled bacterial sample, confirming the assignment of the HISQC spectrum.

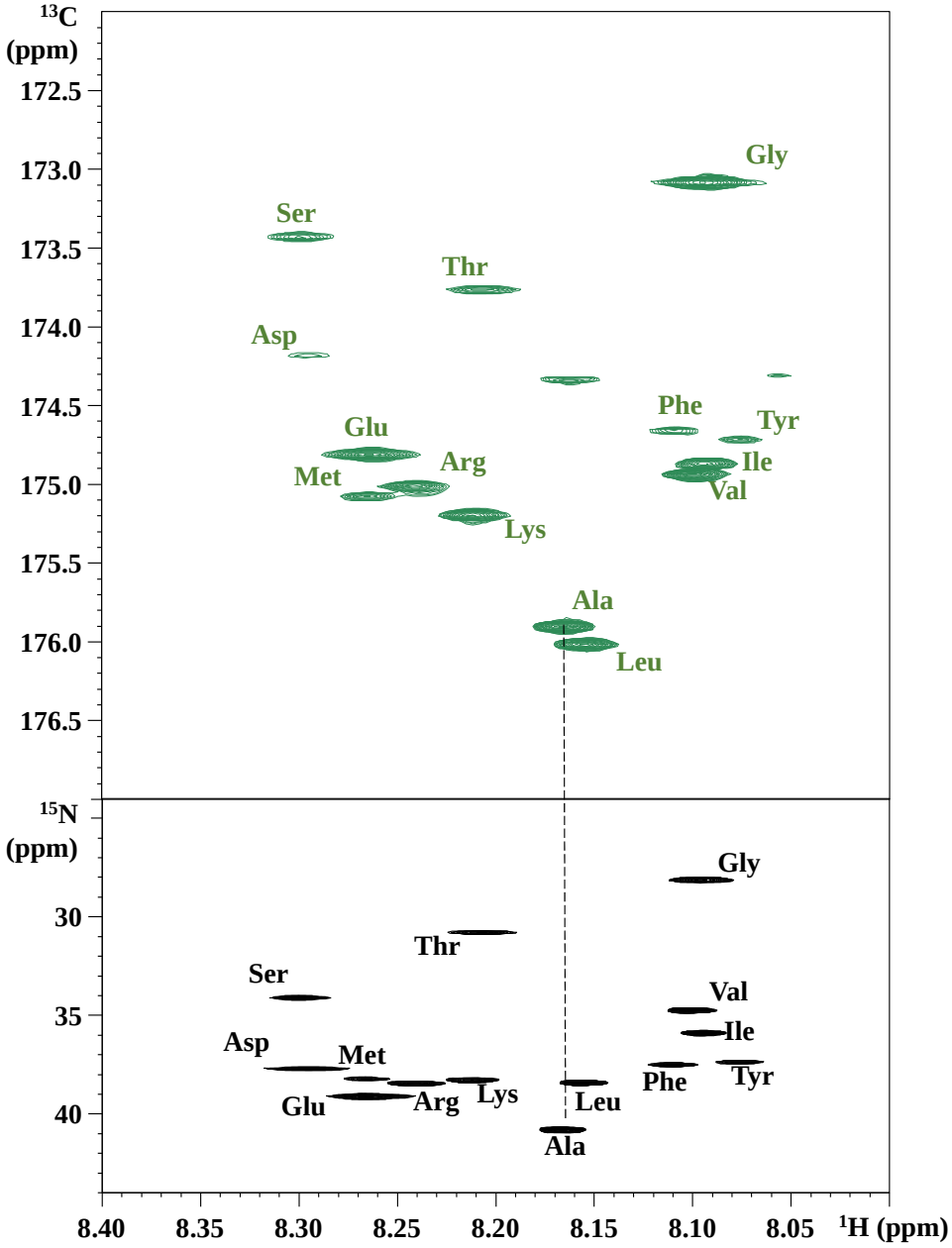

Figure S5-2 (top) ^{1}H, CO plane from the HN(CA)CO experiments with assignment of the different carbonyl resonances in the hydrolyzed U-^{13}C/^{15}N bacterial extract.

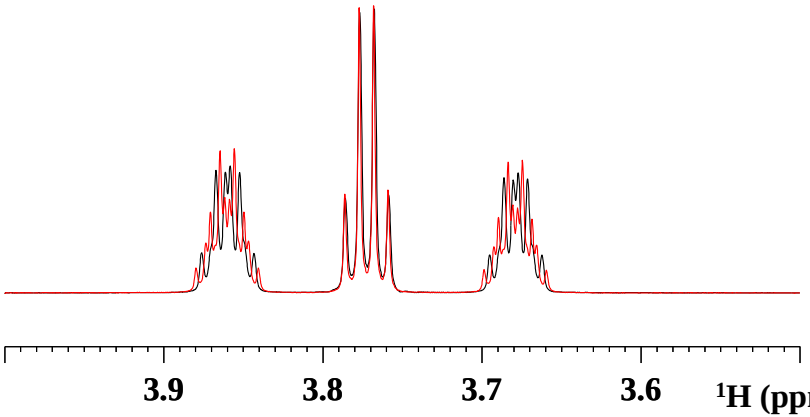

Figure S6-1 1D proton spectrum of U-^{13}C labeled Ala/non-labeled Ala in D_2O, without (red) or with (black) carbonyl decoupling.

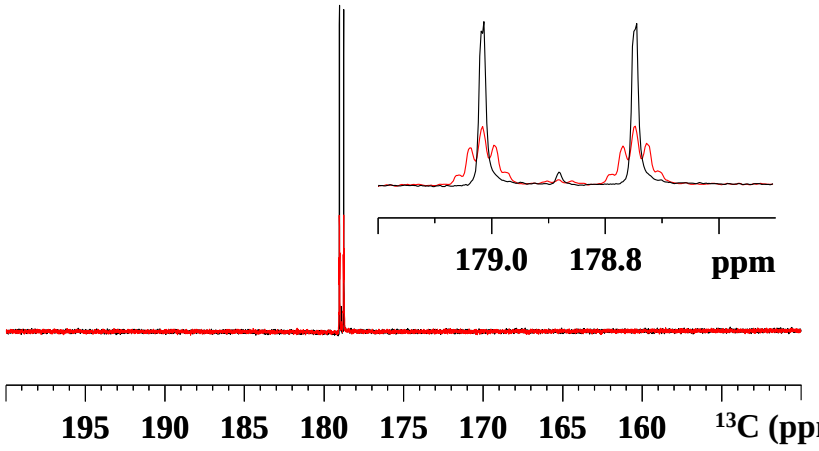

Figure S6-2 1D carbon spectrum of U-^{13}C labeled Ala/non-labeled Ala in D_2O, without (red) or with (black) proton decoupling. The insert shows the fine structure of the carbonyl resonance. Because the pH of this sample is at 7, the chemical shift for the carbonyl is slightly different from that in the hydrolysate at pH 2.0

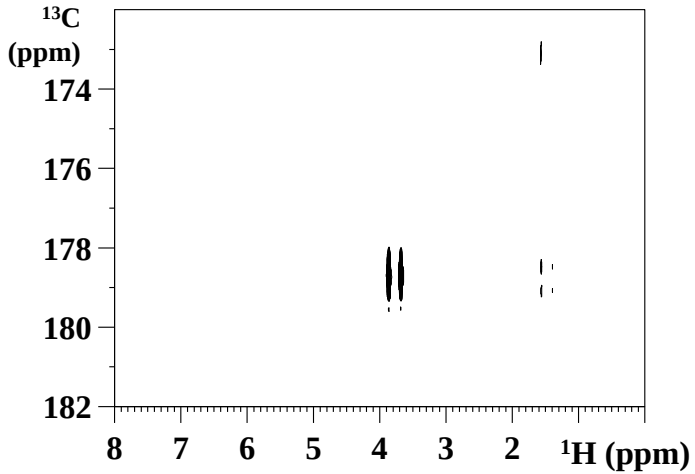

Figure S6-3 1Hα, ^{13}CO correlation with selective CO decoupling in the direct acquisition. A ^{13}Cα 180° pulse in the indirect dimension effectively decouples the Cα-CO coupling.

Figures S6 - (1-3) Measurement of the Hα-CO coupling constant on the ^{13}C labelled Ala sample.

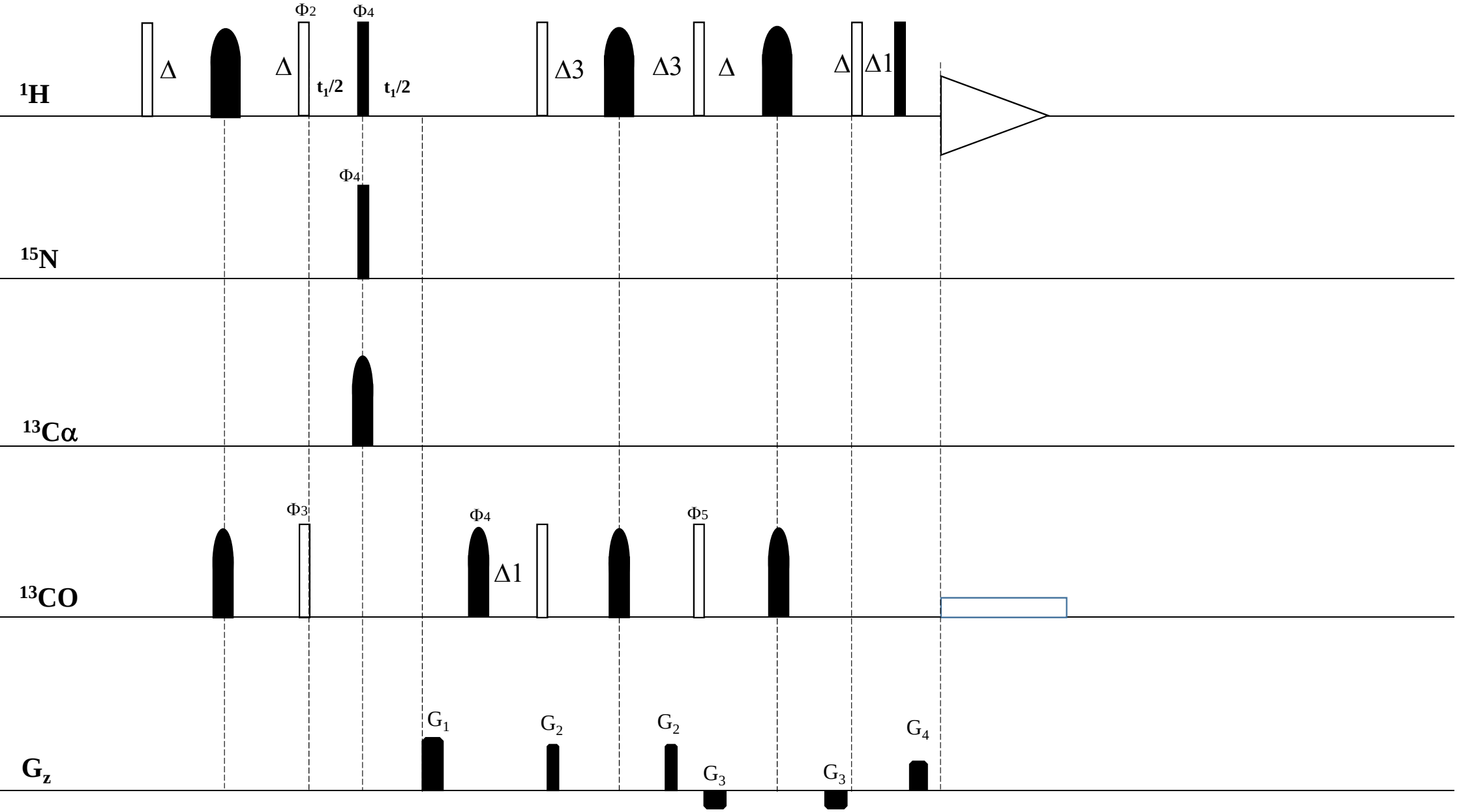

Figure S6-4 Pulse sequence to correlate the Hα and ^{13}CO nucleus within a given amino acid.

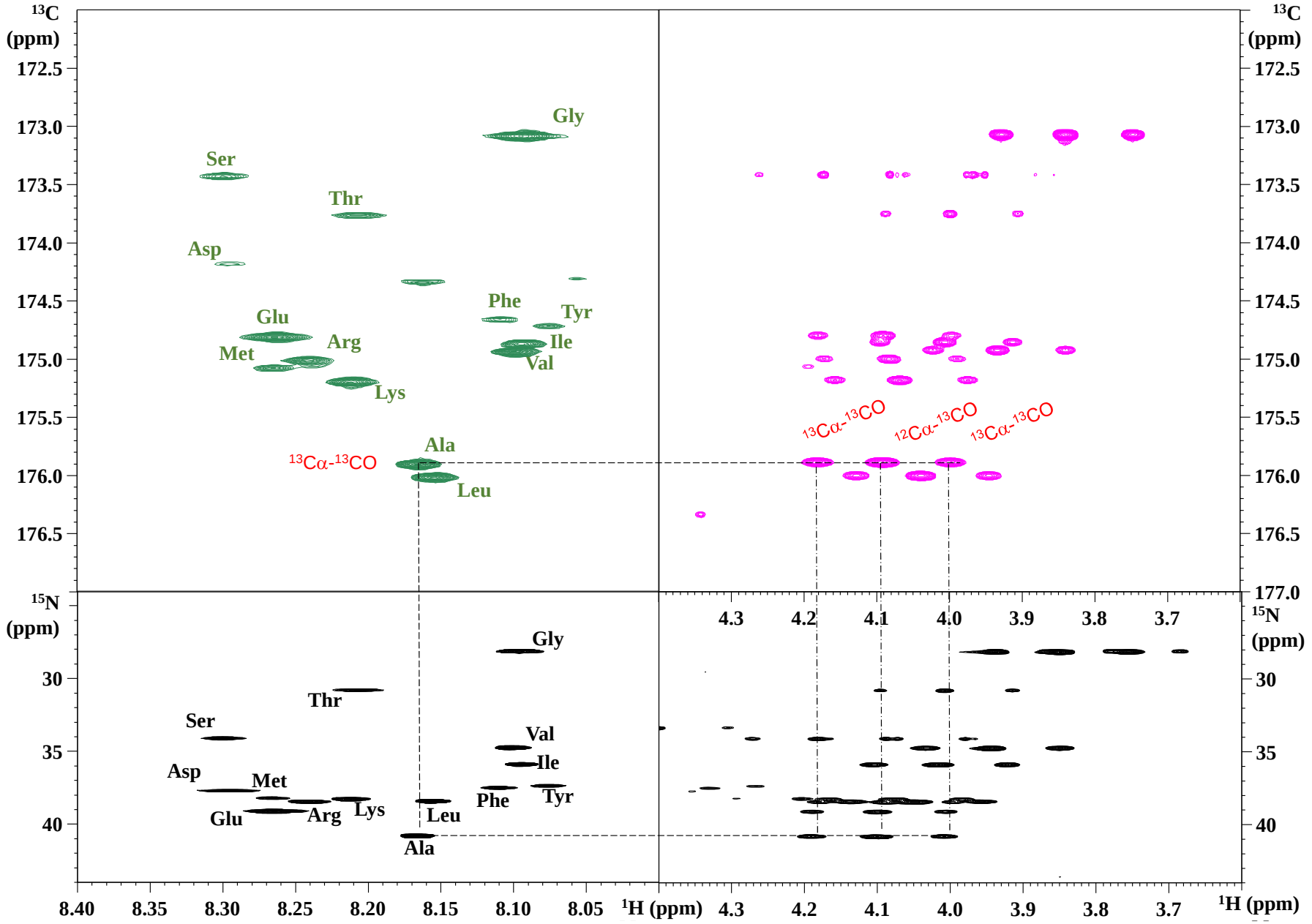

Figure S7 Strategy to assign the resonances of the Hα-CO experiment.

Starting from the assigned HISQC spectrum (bottom, left), the HN(CA)CO spectrum on U-^{13}C labeled sample (top, left) allows to assign all ^{13}CO signals. The HISQC-TOCSY spectrum on a PT-^{13}C labeled sample (bottom, right) gives the Hαcoordinates for the ^{13}Cα/^{12}Cα linked Hα protons of the different amino acids. Coordinates for the different peaks in the Ha-CO spectrum (top, right) are thereby known allowing its full assignment.

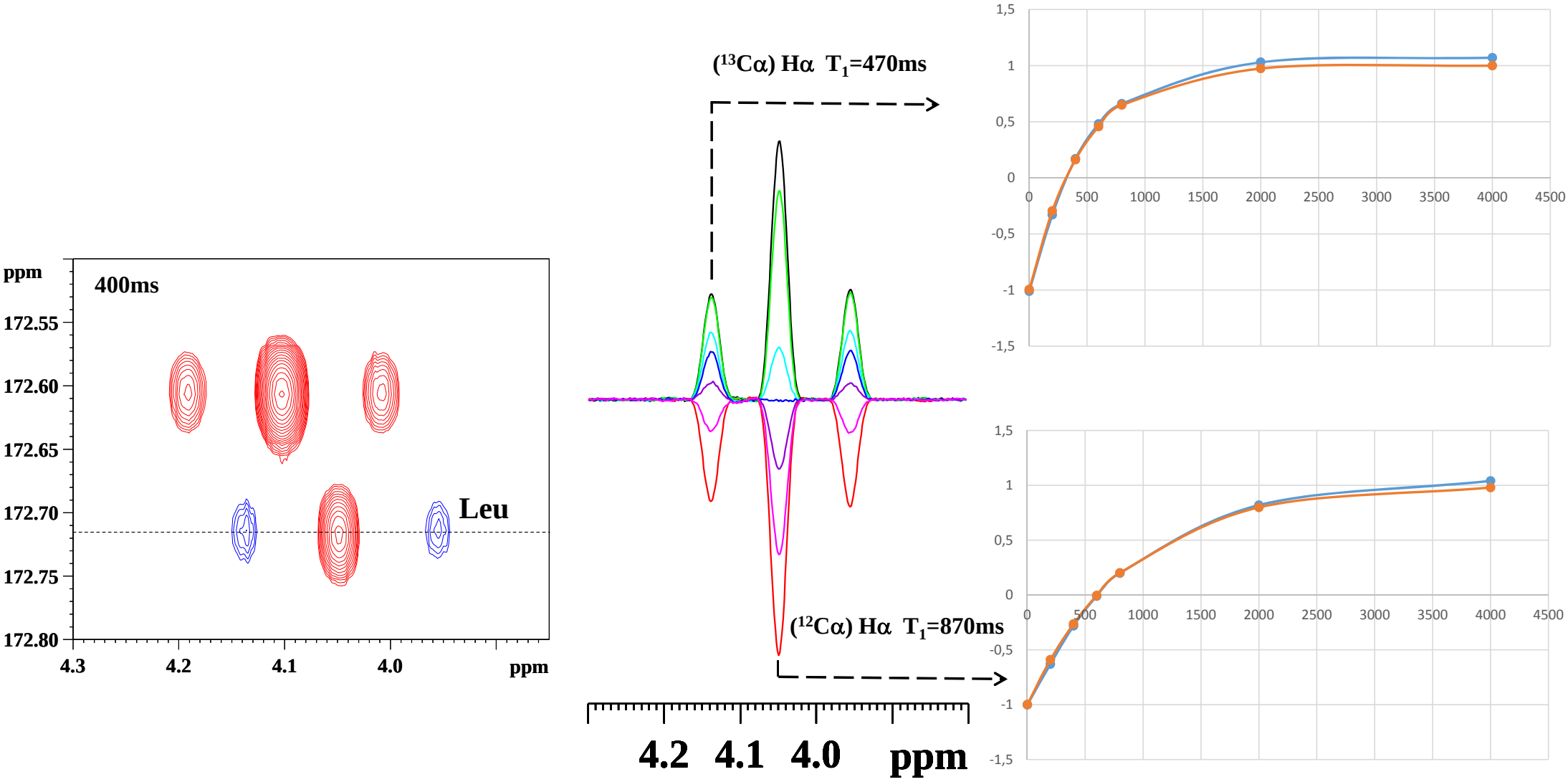

Figure S8-1 Measurement of the T_1 times of the $^{13}C\alpha/^{12}C\alpha$ linked Hα protons for Leu.

The left panel gives a zoom on the inversion-recovery preced Hα-CO experiment with a delay of 400ms. For this delay, the Leu $^{13}C\alpha$ linked Hα proton term is already positive, whereas the $^{12}C\alpha$ linked Hα proton term is still negative.

The middle panel shows the 1D traces extracted for Leu, and the right one the experimental fit to an inversion-recovery curve with delays of 1ms, 200ms, 400ms, 600ms, 800ms, 2s,4s.

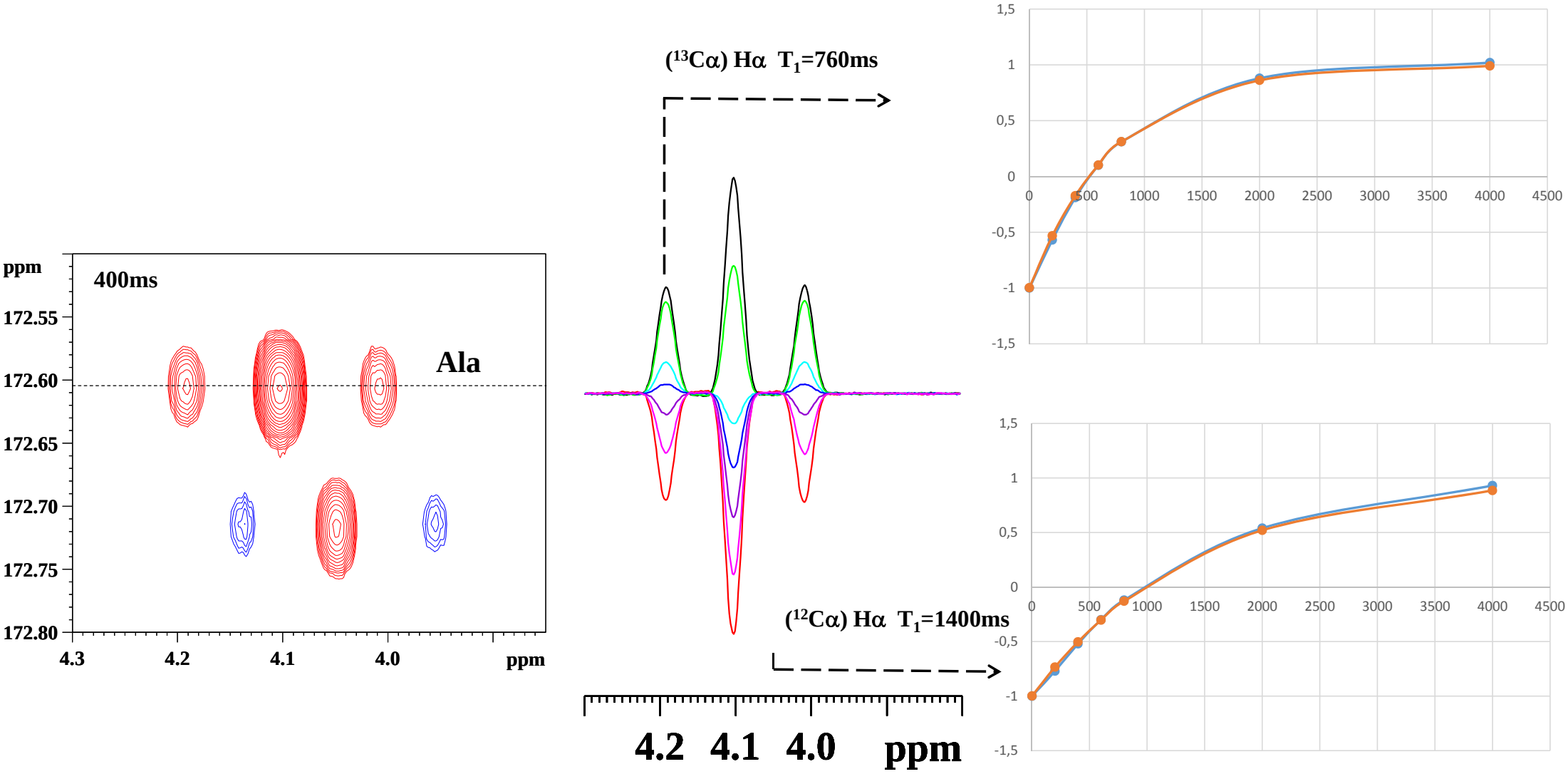

Figure S8-2 Measurement of the T_1 times of the $^{13}C\alpha/^{12}C\alpha$ linked Hα protons for Ala.

The left panel gives a zoom on the inversion-recovery preced Hα-CO experiment with a delay of 400ms. For this delay, both terms are negative.

The middle panel shows the 1D traces extracted for Ala, and the right one the experimental fit to an inversion-recovery curve with delays of 1ms, 200ms, 400ms, 600ms, 800ms, 2s,4s.

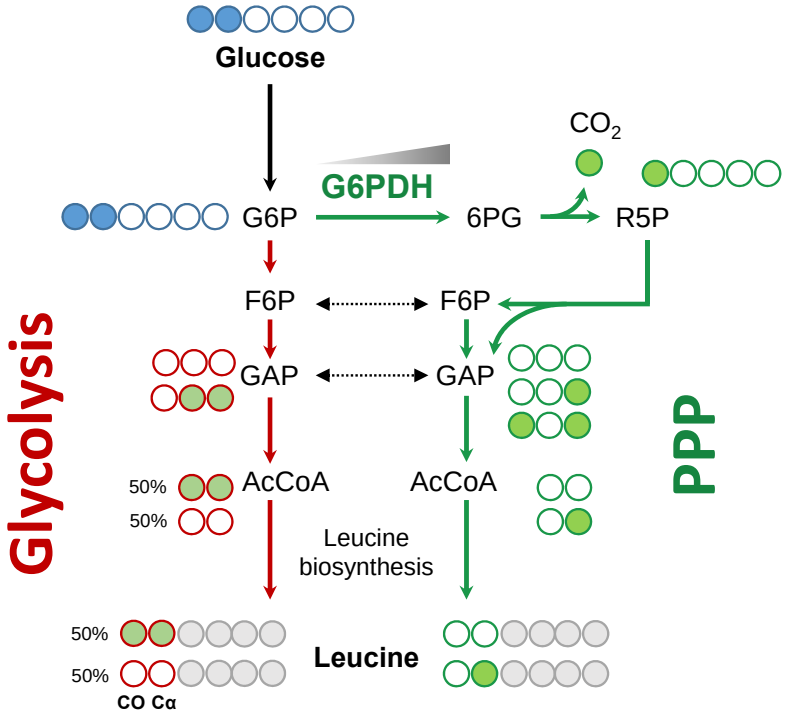

Figure S9. Simplified network of the glycolytic (red) and pentose phosphate (PPP, green) pathways of *E. coli*, showing ^{13}C labelling patterns of some metabolic intermediates and leucine when 1,2-$^{13}C_2$-glucose is used as label input. Empty (filled) circles represent ^{12}C (^{13}C) atoms, and grey circles represent either ^{12}C or ^{13}C atoms

8) References

[1] P. Millard, S. Massou, J.-C. Portais, F. Létisse, *Anal. Chem.* **2014**, *86*, 10288–10295.
[2] M. Wittekind, L. Mueller, *Journal of Magnetic Resonance, Series B* **1993**, *101*, 201–205.
[3] D. R. Muhandiram, L. E. Kay, *Journal of Magnetic Resonance, Series B* **1994**, *103*, 203–216.
[4] A. G. Palmer, J. Cavanagh, P. E. Wright, M. Rance, *Journal of Magnetic Resonance (1969)* **1991**, *93*, 151–170.
[5] T. W.-M. Fan, A. N. Lane, *Progress in Nuclear Magnetic Resonance Spectroscopy* **2008**, *52*, 69–117.
[6] S. Heux, J. Poinot, S. Massou, S. Sokol, J.-C. Portais, *Metab. Eng.* **2014**, *25*, 8–19.